

Dear Prof. Bronstert

We have revised the manuscript according to the suggestions of you and the reviewers. We believe that we have responded adequately to all the comments raised. In particular we have reported “crisp numbers” in line with major previous studies focusing on fitting procedures for weather generators.. The applied methodology is the most common in the academic literature and a section describing this with relevant key references is added to the manuscript. The methodology evaluates whether the simulated precipitation behave like real precipitation with respect to urban-relevant statistics, as done in the manuscript, with relatively simple statistics. We believe that the revised manuscript has been greatly improved due to your qualified input and we look forward to the process ahead. We also agree with the editor that the fitting procedure of WGs is a highly relevant topic for future research.

Best Regards

Hjalte J. D. Sørup and co-authors

## Answers to reviewers as presented in the public discussion

### Reply to Anonymous Referee #1

We very much appreciate the thorough review that has been performed of our manuscript and we will as well as possible answer the questions raised. We acknowledge that the focus and extent of the study is ambitious, and obtaining the fine balance in the manuscript where the right amount of details is reported to make “everything add up” without overloading the reader with details of minor relevance has been a difficult exercise.

Page C1063, first paragraph: As is mentioned the study very much depends on hourly RCM data and the use of a weather generator is exactly chosen to be less dependent on the RCM’s bias and fit to present observations. The two ENSEMBLES data sets used in hourly resolution are obtained through direct contact to the groups who produced them: the RACMO-ECHAM through KNMI as mentioned in the acknowledgements and the HIRHAM-ECHAM through DMI who is co-authoring the paper. This last point will be added to the acknowledgements. The four high resolution RCMs come out of a research project and Mayer et al. (2015) is indeed only the validation of the reference runs against observations. However, this reference is used, as it is the same models with the same configurations and grids which are run under the two RCP scenarios used in the present study.

Page C1063, first paragraph: We will add a small discussion to the manuscript on the reliability of hourly RCM data along with a discussion of the use of change factors to be less dependent on this reliability.

Page C1063, second paragraph: The paper’s focus on extremes and their change in the future is indeed important and validation of methods also. The weather generator as such, as well as the individual measures used to describe the extremes, are all validated in literature as referenced in the manuscript. For the novelty of using the weather generator with abundant data on very small scale we lack instruments for thorough validation. As the observational data set is very unevenly distributed and lacks data in many points for extensive periods we do not expect the weather generator data and the observational data to fit each other perfectly. What we expect is merely an approximate fit (but for the parameters, not only the average rainfall). Thus, we do not expect that a Kolmogorov-Smirnov test (or the like) would give any positive result if applied on any of the points in the model as we do not expect the extremes to happen at the exact same spatial locations as in the original data set.

Page C1063, second paragraph and page 1065 fourth paragraph: We acknowledge that Figure 5 does not provide enough information to discuss the fit of the model and will replace it with a figure showing the density plots of the normalized errors for the different parameters, to highlight that the density is higher near the 1:1 line of the present Figure 5 and to guide the discussion on how accurate (unbiased) the model is and on how large the variance therefore is.

Page C1063, second paragraph and page 1065, comment starting with 2576, 11: With respect to Figure 6 it was not convincing that the model is site specific. Again, the differences between the observational data set and the weather generator output should result in differences and Figure 6 shows that we have the same trends. Also, here we lack rigorous statistics to describe what would constitute an adequate fit given the above mentioned differences in the data set and expectations.

This study is very much a proof of concept of the fact that we are able to use a weather generator for a purpose it was not developed for in an area where we need methods to generate finer resolution time series data for possible future climates.

### *Answers to the more specific questions.*

Page C1063, second last paragraph: Whether the manuscript would have been better told in two parts is not a discussion we want to open up at this stage. We believe that the scientific value of having it all together serves a purpose and, hence, we have collected the results into the present manuscript.

Page C1063, last paragraph: Applying change factors directly to time series is definitely an easy solution but also a solution, which we believe will result in unrealistic time series, as we know that the mean changes and changes to extremes are not necessarily the same. Especially in the summer months we expect less rainfall on average but an increase in the extreme amounts and independently on the change factor relationship chosen, this would result in either too much rainfall in total or too small extremes in general. The weather generator methodology is an approach adopted in an attempt to overcome these issues and produce time series that are realistic in more aspects than just extremes or just mean rainfall.

Page C1064, second paragraph: The term “change factor” is indeed used ambiguously in the manuscript, and we will change one of the uses for something just as appropriate.

Page C1064, third paragraph: The naming of the weather generator in the manuscript is interesting. As we see it the fact that it is a (ST)NSRP weather generator is important and described in the methodology but the same kind of study could just as well have been carried out with other spatio-temporal weather generators where relevant properties of rainfall are described and thus we believe that the generic WG for weather generator is well justified as naming convention in the manuscript.

Page C1064, fourth paragraph: The observational data are treated as stationary in this manuscript and no climate trend is identified within the observational period for this study event though there could potentially be one as pointed out by Gregersen et al (2013). We do not believe that this causes any major effects on the resulting model, as the area is very homogeneous with respect to the input data.

Page C1064, line starting with 2568, 7 and 2571, 3 and 4: We will change the manuscript order to avoid discussions on aspects that are not presented adequately beforehand.

Page C1064, line starting with 2567 and 2571, 5: The core components of the weather generator and the calculations of appropriate change factors have been developed by the Newcastle group (Burton et al.) and as such we do not wish to reproduce their findings here. The first issue is really well described in several papers and will be thoroughly referenced to guide the reader for the best places to obtain this information. The second issue is described in another Burton et al. (2010) paper than the one referenced, hence the confusion; this will be corrected in the manuscript.

Page C1064, line starting with 2570, 21: We will add a section discussing the calibration and simulation times of the WG. In general the calibration can be cumbersome, but the simulation is very swift (even though the actual “writing to text files” part can take time if many hundreds of points are included in the simulation).

Page C1064, line starting with 2568, 12: Whether intensity and duration are correlated in general is an interesting issue that we do not discuss in this manuscript. However, IDF curves do not say anything about the actual event lengths and about their mean intensities. A 1 hour maximum value might well originate in a

much longer event where the 3 or 6 hour maximum values were not extreme. And on the rain cell level where the weather generator operates the picture is even more unclear, particular since the extremes are the product of multiple cells overlapping in time and space. Hence, it is not a discussion we believe will enhance the manuscript and we do not plan to incorporate it in the manuscript.

Page C1064, line starting with 2568, 25: As the CGD data set is only used to compute monthly means for the application area we believe that the length of data is not a problem for this study.

Page C1065, line starting with 2574, 1: The unconditional spatial correlation is thoroughly described in Mikkelsen et al. (1996). The word 'unconditional' reflects that the methodology takes into account that the events at the compared stations are actually happening at the same time and that all the events registered at times where both stations were working but only registered at one station are also weighed into the correlation.

Page C1065, line starting with 2575, 6: The fitting is a bit unstable but within small realistic bounds and mostly for the parameter that controls the time at which the first cell arrives after a storm is initiated. All the results show that cells arrive more or less immediately after the start of the event. The results between different realizations of the weather generator (WG1-10) show clearly that this fitting behaviour does not influence the results to any extent.

Page C1065, line starting with 2577, 1: The 100 year event shown in Figure 7 is a product of an extrapolation of data using a PDS approach and a GPD model. As such there is no direct link to the discrepancies observed in Figure 5 and as we will replace Figure 5 with a more appropriate one this picture should be clearer with the new Figure 5.

### **Reply to Søren Thorndahl**

Thank you very much for the thorough review.

Page C1750, paragraph two: We will add further discussion and references on the appropriate temporal scale of urban rainfall in a climate change context, but even though finer temporal scale data would be very beneficial in urban hydrology the link to climate change and the RCM data available would be worsened markedly.

Page C1750, paragraph three: Inclusion of IDF curves were considered in the manuscript writing process but the final choice was to include the relative measures reported in Figure 11. This is essentially the same data, but normalized against the IDF curve for present data. Due to the double-logarithmic axes used in IDF curves it was very difficult to discuss differences and the present Figure 11 was thought to better support this.

Page C1750, paragraph four: The focus has been solely on extremes as this aspect has been assessed to be of most importance for the direct dimensioning of urban water collection systems. With respect to CSO's the definition used in this study includes events that should be frequent enough to include a fairly large part of the CSO causing events, at least in many Danish contexts. Also in waste water treatment plant operations the extremes are very important in the operations as the hydraulic capacity will also be determined in a design phase based on events that are included in the definition of extremes of this study.

Page C1750, paragraph five: For the novelty of using the weather generator with abundant data on very small scale we lack instruments for thorough validation. As the observational data set is very unevenly distributed and lacks data in many points for extensive periods we do not expect the weather generator data and the observational data to fit each other perfectly. What we expect is merely an average fit (but for the parameters, not only the average rainfall). Thus, we do not expect that a Kolmogorov-Smirnov test (or the like) would give any positive result if applied on any of the points in the model as we do not expect the extremes to happen at the exact same spatial locations as in the original data set.

Page C1750, paragraph six and eight: On the question whether the weather generator could have been calibrated differently or better the short answer is: Yes – probably. And this of course relates to the subjectivity of the weighing factors. The weighing factors are, as stated in the manuscript, based on knowledge about rainfall and a subjective assessment of which elements are considered important in that context. Others would have chosen other weight factors resulting in different calibrations; some of them potentially better. We have not invested time in pursuing the best possible fit; we merely see this study as a proof-of-concept that it is possible to use this model framework at much different scales than what is usually seen. Thus, satisfactory in this context is that we from our knowledge of rainfall can set up a weighing scheme that results in a calibration that again result in data that actually behaves similarly to the input.

Page C1750, fourth last paragraph: We will specify in Figure 3 that the isohyets are 3 mm.

Page C1750, last paragraph: For Figure 4 we will add a discussion on the yearly variation where appropriate.

Page C1751, first and second paragraphs: We acknowledge that Figure 5 does not provide enough information to discuss the fit of the model and will replace it with a figure showing the density plots of the normalized errors for the different parameters, to highlight that the density is higher near the 1:1 line of the present Figure 5 and to guide the discussion on how accurate (unbiased) the model is and on how large the variance is.

Page C1751, third paragraph: As stated in the methodology section the evaluations are based on a PDS approach and a Generalized Pareto Distribution model fitted to data (both observation and weather generator data) and, no, we do not have 100 years of data and it is therefore an extrapolation, but the 100 year return period is interesting in urban water management as cloudburst management is becoming increasingly relevant. The typo in the text with the 50 year event will be corrected.

Page C1751, fourth paragraph A confidence interval for the estimation of the SVK IDF curve will be added to Figure 7 to show the relative closeness of the WG fits.

## List of changes made to the manuscript

P1L5: Correction of affiliation.

P1L7: Correction of affiliation.

P2LL10-13: Clarification of sentence and addition of relevant references.

P2L20: Addition of reference.

P3LL2-4: Addition of references.

P3L17: Clarification of Burton 2010 reference as requested by Reviewer 1.

P3LL25-27: Clarification of choice of temporal scale as requested by S. Thorndahl.

P5L9: deletion of “/”.

P5LL19-30: Minor corrections and clarification of the origin of 1h HIRHAM data as requested by Reviewer 1 and Editor.

P6LL10-11: Proper reference added on the description of the weather generator, further clarification of Burton 2010 reference as requested by Reviewer 1.

P6LL14-22: Movement of paragraph from after bullet points as suggested by reviewer 1. Clarification of Burton 2010 reference as requested by Reviewer 1.

P7L26: Clarification of Burton 2010 reference as requested by Reviewer 1.

P8LL12-14: Sentence added to clarify the reason behind the chosen weighing scheme as requested by S. Thorndahl.

P8LL26-32: Sentence added to clarify why the evaluation of the model is done in the way it is with proper referencing to the relevant papers as requested by both reviewers and Editor.

P9LL6-10: Sentence added on actual simulation times as suggested by Reviewer 1.

P9LL11-13: Methodology for the normalized error added in response to the change of Figure 5.

P9LL15-22: Minor clarifications regarding the difference between “change factors” and “climate factors” as requested by reviewer 1. Clarification of Burton 2010 reference as requested by Reviewer 1.

P10:LL16-17: All durations considered listed and there threshold relationship clarified as requested by S. Thorndahl.

P11L10: Minor clarifications regarding the difference between “change factors” and “climate factors” as requested by reviewer 1.

P13LL23-32 and P14LL1-6: Section rewritten in response to reporting of normalized errors in Figure 5 and addition of the new Table 4 in response to the request for “crisp numbers” raised by both reviewers and the Editor.

P14L7: “on” changed to “in”.

P14L23: 100 replace 50 as pointed out by Reviewer 1.

P14L25: Section extended due to changes made to Figure 7 in response to comment by S. Thorndahl.

P15L27: Minor clarifications regarding the difference between “change factors” and “climate factors” as requested by reviewer 1.

P16L28: Minor clarifications regarding the difference between “change factors” and “climate factors” as requested by reviewer 1.

P19L18-19: Clarification of the origin of 1h HIRHAM data added to the acknowledgement in response to comments by Reviewer 1 and Editor.

P30: Table 4 (the two following tables shift up numbering): Table added in direct response to the wish for “crisp numbers” on the fit of the WG to the SVK data requested by both reviewers and the Editor.

P35: Figure 3: Specification of the level between isohyets specified in the caption as requested by S. Thorndahl.

P37-38: Figure 5: Figure changed to show normalized error instead of point clouds as a response to comments by Reviewer 1.

P40: Figure 7: Confidence interval for the SVK data set added to figure to better illustrate the relative fit of the WGs as a response to comment by S. Thorndahl.

P43: Figure 10: Minor clarifications regarding the difference between “change factors” and “climate factors” in the caption as requested by Reviewer 1.

References: Several references added.

Numbering of Equations and Tables are shifted due to one new table and one new equation.

1 Downscaling future precipitation extremes to urban hydrology  
2 scales using a spatio-temporal Neyman-Scott weather  
3 generator

4 H. J. D. Sørup<sup>1,2</sup>, O. B. Christensen<sup>2</sup>, K. Arnbjerg-Nielsen<sup>1</sup> and P. S. Mikkelsen<sup>1</sup>

5 [1]{Urban Water [Engineering](#) Section, Department of Environmental Engineering, Technical  
6 University of Denmark, Lyngby, Denmark}

7 [2]{[Section for Climate and Arctic Danish Climate Centre](#), Danish Meteorological Institute,  
8 Copenhagen, Denmark}

9 Correspondence to: H. J. D. Sørup (hjds@env.dtu.dk)

10 **Abstract**

11 Spatio-temporal precipitation is modelled for urban application at 1-hour temporal resolution  
12 on a 2 km grid using a Spatio-Temporal Neyman-Scott Rectangular Pulses weather generator  
13 (WG). Precipitation time series for fitting the model are obtained from a network of 60  
14 tipping-bucket rain gauges irregularly placed in a 40 by 60 km model domain. The model  
15 simulates precipitation time series that are comparable to the observations with respect to  
16 extreme precipitation statistics. The WG is used for downscaling climate change signals from  
17 Regional Climate Models (RCMs) with spatial resolutions of 25 km and 8 km respectively.  
18 Six different RCM simulations are used to perturb the WG with climate change signals  
19 resulting in six very different perturbation schemes. All perturbed WGs result in more  
20 extreme precipitation at the sub-daily to multi-daily level and these extremes exhibit a much  
21 more realistic spatial pattern than what is observed in RCM precipitation output. The WG  
22 seems to correlate increased extreme intensities with an increased spatial extent of the  
23 extremes meaning that the climate-change-perturbed extremes have a larger spatial extent  
24 than those of the present climate. Overall, the WG produces robust results and is seen as a  
25 reliable procedure for downscaling RCM precipitation output for use in urban hydrology.

26 **1 Introduction**

27 Pluvial flooding of urban areas is often caused by very local extreme precipitation at sub-daily  
28 temporal scale (Berndtsson and Niemczynowicz, 1988, Schilling, 1991). Traditionally,  
29 historical gauge measurements of precipitation at minute-scale temporal resolution are thus  
30 used as input to design and analysis of urban water infrastructure (Mikkelsen et al., 1998,



1 Madsen et al., 2009, Arnbjerg-Nielsen et al., 2013). Climate change is however expected to  
2 change the occurrence rate and magnitude of extreme events causing urban pluvial flooding  
3 (Fowler and Hennessy, 1995; Larsen et al., 2009; Olsson et al., 2009, Sunyer et al., 2014), and  
4 high-resolution input time series representing future climates are therefore needed. Even  
5 though the overall qualitative features of precipitation are reproduced realistically by regional  
6 climate models (RCMs) (Christensen and Christensen, 2007) they are, however, not able to  
7 capture the very fine-scale spatio-temporal features of precipitation satisfactorily and yield  
8 output that is too spatially correlated (Tebaldi and Knutti, 2007; Gregersen et al., 2013). To  
9 overcome this, either dynamic downscaling with climate models has to operate at much finer  
10 scales [in order to properly describe convective precipitation dynamics](#) (Kendon et al., 2014;  
11 Mayer et al., [accepted2015](#)) or further statistical downscaling of the climate model output has  
12 to be performed ([Olsson and Burlando, 2002](#); Wood et al., 2004; [Cowpertwait, 2006](#); [Molnar](#)  
13 [and Burlando, 2008](#); Willems et al., 2012; Sunyer et al., 2012; Arnbjerg-Nielsen et al., 2013).  
14 Fine scale dynamic downscaling is computationally extremely expensive and statistical  
15 downscaling is therefore often favoured (Maraun et al., 2010). Several approaches exist  
16 within statistical downscaling, each with its pros and cons (Wilks and Wilby, 1999; Willems  
17 et al., 2012; Arnbjerg-Nielsen et al., 2013). In the present study a stochastic weather generator  
18 (WG) is used for statistical downscaling.

19 WGs can take different forms (Vrac et al., 2007; Burton et al., 2008; Arnbjerg-Nielsen and  
20 Onof, 2009; Chen et al., 2010; Cowpertwait et al., [2006](#); 2013) but they generally work by  
21 analysing observed precipitation (and possibly other weather related variables) and use the  
22 obtained statistics to create artificial stochastic precipitation (or weather) time series that  
23 replicate the behaviour of the observations with respect to these statistics (Maraun et al, 2010,  
24 Sunyer et al., 2012). Perturbation of the WG to yield output time series representing future  
25 climates is then possible by application of climate change factors calculated from output from  
26 RCMs (operation at too large space-time scales) to relevant parameters of the WG (that  
27 operates at the right space-time scale).

28 Several WGs exist that model precipitation as a stochastic point process where the given  
29 observations are considered single realisations of an underlying precipitation process  
30 (Waymire and Gupta 1981). Rodríguez-Iturbe et al. (1987a,b) developed the stochastic point  
31 process models in a way to better characterise and describe the precipitation process at the  
32 event level. Implementations of the stochastic point process models for spatio-temporal

1 precipitation seem to work satisfactorily at a temporal resolution of one hour or higher  
2 (Cowpertwait and O'Connell, 1997; Burton et al., 2008; 2010; Cowpertwait et al., [2006:](#)  
3 2013). Also, downscaling to finer resolution than one hour is inherently problematic as the  
4 scaling properties change below this point (Nguyen et al., 2002; [Molnar and Burlando, 2008](#)).  
5 Thus, for downscaling of extreme precipitation at sub-daily level and subsequent application  
6 of climate change signals from climate models, stochastic weather generators implementing  
7 stochastic point process models seem useful (Cowpertwait, 1998; Furrer and Katz, 2008;  
8 Hundecha et al., 2009; Verhoest et al., 2010; Sunyer et al., 2012). The trade-off is that the  
9 models do not involve rainfall movement and, hence that the spatio-temporal scale of the  
10 model has to be such that rainfall movement is not the main descriptor of the spatial rainfall  
11 pattern.

12 At the daily level, the Neyman-Scott Rectangular Pulses (NSRP) and the Spatio-Temporal  
13 Neyman-Scott Rectangular Pulses (STNSRP) models (Burton et al., 2008; 2010; Cowpertwait  
14 et al., 2013) have shown good skill in downscaling point precipitation extremes. This applies  
15 for individual gauges (Sunyer et al., 2012) as well as for spatially averaged precipitation  
16 covering large areas considered as having a uniform climate described by relatively few  
17 gauges (e.g. 5 gauges for a 4000 km<sup>2</sup> basin in the Pyrenees (Burton et al., 2010a) and 3  
18 gauges used to calibrate a regional model covering a catchment of 342 km<sup>2</sup> in the Basque  
19 Country (Cowpertwait et al., 2013)). This is however inadequate in urban hydrology where  
20 the rainfall dynamics causing effects under study occur on much smaller time and space  
21 scales.

22 In the present study, the STNSRP weather generator (WG) in the form of the software  
23 package RainSim (version 3.1.1, Burton et al., (2008)) is used in a new, urban hydrology  
24 context focusing on much smaller space and time scales than what has been done in previous  
25 studies. [Due to the limitations in scalability of both RCM model output and precipitation  
26 measurements discussed above a temporal resolution of 1 hour is adopted, even though a  
27 higher resolution would be preferable from an urban hydrology perspective.](#) It is fitted to  
28 hourly data from 60 rain gauges from a dense rain gauge network in Denmark and used to  
29 generate synthetic precipitation data series on an equally dense grid covering approximately  
30 2400 km<sup>2</sup>. The synthetic precipitation data is then evaluated with respect to its applicability  
31 for urban hydrological purposes. A 1-hour temporal resolution on a 2 km grid is chosen as  
32 realistic and sufficient performance scales of the model for fine-scale precipitation data in

1 urban hydrology. The evaluation of the WG is done from an engineering perspective with  
2 respect to its ability to reproduce rainfall features relevant for urban hydrological modelling.

3 We will thus focus on:

- 4 • the WG's ability to produce realistic extreme event intensities at point scale
- 5 • the WG's ability to reproduce the seasonal distribution of extreme events at point  
6 scale
- 7 • the WG's ability to reproduce small scale spatio-temporal correlation structures  
8 of the extreme events

9 This study uses the presented WG to analyse climate change in precipitation at scales  
10 comparable to the observational data sets traditionally used today for urban water  
11 infrastructure design and analysis. The WG is perturbed with climate change information  
12 obtained from a collection of temporal high resolution RCMs. Six RCM runs using three  
13 different RCMs, driven by three different GCMs and covering three different emission  
14 scenarios (ranging from average to very high emissions) are included in the analysis and four  
15 of the RCM runs are run as high resolution models at an 8 km grid. Finally, climate change at  
16 urban scale is assessed based on the perturbed WG output.

## 17 **2 Data and weather generator**

### 18 **2.1 Data representing present conditions**

19 The model area is a 40 by 60 km region covering the North-Eastern part of Zealand  
20 (Denmark) including Copenhagen, see Figure 1. This study uses two different observational  
21 data sets; Table 1 summarises their main characteristics.

22 The area is highly urbanised and has a dense but irregular network of rain gauges designed  
23 and used for urban hydrology applications. The main observational precipitation data set,  
24 SVK (abbreviation for *Spildevandskomiteen*, the Water Pollution Committee of the Society of  
25 Danish Engineers) is obtained from this dense network of high-resolution tipping bucket rain  
26 gauges (Jørgensen et al., 1998; Sunyer et al., 2013). Data from 60 stations that have been  
27 active between 2 and 34 years in the period 1979 and 2012 are included in the analysis; see  
28 Figure 1 for locations within the study area. Figure 2 shows the temporal development of  
29 (top) the number of active stations and (middle) the average distance between nearest  
30 neighbouring stations through the measuring period, and Figure 2 (bottom) shows the  
31 distribution of record lengths by 2012. Generally, there has been an increase in the number of  
32 stations and a densification of the network over the years. Some studies impose a minimum

1 length of the time series to be included in regionalisation studies, e.g. Madsen et al. (2009),  
2 but in this study the cross-correlation is of key interest and hence all gauges are included in  
3 the analysis regardless of their record length. The original data resolution is 1 min and 0.2 mm  
4 but for the present study, data is aggregated to hourly time series. This data set is used to  
5 estimate (or calibrate, or fit) most of the parameters of the WG.

6 The second observational data set included in the analysis is referred to as the Climate Grid  
7 Denmark (CGD) (Scharling 2012). It comprises spatially averaged daily data in a uniform 10  
8 km grid for all of Denmark from 1989 to 2010 inclusive, cf. Figure 1. This data is generated  
9 based on a national network of gauges with 27 gauges within the study site (Scharling 1999)  
10 and is only used to estimate the spatial component in the WG.

11 Finally, a third data set is the output from the applied weather generator (WG). A total of 10  
12 data sets comprising sets of 50 years' time series in the 2 km grid (as shown on Figure 1) are  
13 simulated as output from the WG. These data sets are used to corroborate the WG by refitting  
14 and rerunning it, evaluating the output variability and comparing the output statistics to those  
15 of observations.

## 16 **2.2 Regional climate model data**

17 Precipitation output from six different RCM runs is used in this study, see Table 2. Two of the  
18 model runs are identical to the ones used by Gregersen et al. (2013), namely the two SRES  
19 A1B scenarios ~~driven driving by~~ the RCM RACMO (version 2.1, Meijgaard et al., 2008) and  
20 the RCM HIRHAM (version 5, Christensen et al., 2006), which are both driven by the GCM  
21 ECHAM5 (Roeckner et al., 2003) and are part on the ENSEMBLES project (van der Linden  
22 and Mitchell, 2009). Both have a spatial resolution of 25 km and a temporal output resolution  
23 of 1 hour. These were the two ENSEMBLES runs we had available through personal contacts  
24 for the present study at true 1-hour resolution. The more generally available data series with  
25 only daily maximum 1-hour intensity are not sufficient for the employed downscaling  
26 procedure. The four other simulations used in this study are run with the RCM HIRHAM  
27 driven by the GCM EC-EARTH (Hazeleger et al., 2012) and the RCM WRF (Skamarock et  
28 al., 2005) driven by the GCM NorESM (Bentsen et al., 2013). The four simulations use the  
29 RCP 4.5 and RCP 8.5 scenarios (van Vuuren et al., 2011), see Table 2. The spatial resolution  
30 of these simulations is 8 km and the output frequency is 1 hour (Mayer et al., accepted2015).  
31 The simulations were carried out as part of the research project RiskChange

1 (www.riskchange.dhigroup.com). The SRES A1B and RCP 4.5 scenarios are considered  
2 comparable moderate forcing scenarios whereas the RCP 8.5 scenario is a very strong forcing  
3 scenario.

4 As in Gregersen et al. (2013), climate change is considered uniform for all land cells over  
5 Denmark; this results in 87 considered grid cells for the ENSEMBLES simulations and 648  
6 for the RiskChange simulations.

### 7 **2.3 Weather generator**

8 The RainSim WG describes the spatio-temporal rain field as discs of rain (rain cells) with  
9 uniform rain intensity that temporarily occur and overlap in space and time to produce output  
10 that realistically describe the statistical properties of precipitation ([see Burton et al. \(2010a\)](#)  
11 [for a thorough description of the weather generator](#)). As the calibration data set consists of  
12 point observations, the time series from the simulations are not grid cell averages but strictly  
13 comparable to what a gauge would have measured if present in a grid point.

14 [A uniform Poisson process governed by  \$\lambda\$  describes the storm occurrences. For each storm a](#)  
15 [random number of rain cells are produced, which occur at independent time intervals after the](#)  
16 [storm origin and where the time intervals follow an exponential distribution with parameter  \$\beta\$ .](#)  
17 [A uniform spatial Poisson process governed by  \$\rho\$  describes the density of the rain cells in](#)  
18 [space. The cell radii are randomly drawn from an exponential distribution described by  \$\gamma\$ , and](#)  
19 [the duration and intensity of each rain cell is independent and follows an exponential](#)  
20 [distribution with parameters  \$\eta\$  and  \$\zeta\$ , respectively. The rain intensity at a given point is](#)  
21 [therefore the sum of all overlapping rain cell intensities at a given time. In all, seven](#)  
22 parameters describe the WG (Burton et al., ~~2008~~; 2010a):

- 23 •  $\lambda^{-1}$ , the mean waiting time between storm origins (in hours)
- 24 •  $\beta^{-1}$ , the mean waiting time for rain cell origins after storm origin (in hours)
- 25 •  $\eta^{-1}$ , the mean duration of rain cells (in hours)
- 26 •  $\rho$ , the spatial density of rainfall cell centres (cells per km<sup>2</sup>)
- 27 •  $\zeta^{-1}$ , the mean intensity of the rain cells (in mm/h)
- 28 •  $\gamma^{-1}$ , the mean radius of the rain cells (in km)
- 29 •  $\Phi$ , the non-homogeneous intensity scaling field describing how the mean  
30 monthly rainfall intensity varies in space within the model area (-)

~~A uniform Poisson process governed by  $\lambda$  describes the storm occurrences. For each storm a random number of rain cells are produced, which occur at independent time intervals after the storm origin and where the time intervals follow an exponential distribution with parameter  $\beta$ . A uniform spatial Poisson process governed by  $\rho$  describes the density of the rain cells in space. The cell radii are randomly drawn from an exponential distribution described by  $\gamma$ , and the duration and intensity of each rain cell is independent and follows an exponential distribution with parameters  $\eta$  and  $\xi$ , respectively. The rain intensity at a given point is therefore the sum of all overlapping rain cell intensities at a given time (Burton et al. 2008; 2010).~~

The non-homogeneous intensity scaling field,  $\Phi$ , is a proxy for the spatial variation of mean monthly precipitation and is used for relative scaling of the precipitation in space; for this study it is interpolated from the CGD data set using inverse distance weighting. Regional modelling of short-duration extreme precipitation for Denmark using the SVK data set has shown that the only significant parameter that can explain the geographical variation of point extremes statistically is the corresponding mean annual precipitation (Madsen et al., 2002; 2009). Thus, taking  $\Phi$  as the only spatially varying parameter in the WG, and as such the only parameter describing spatial differences within the WG, is considered to be an acceptable approximation. The actual spatial variation of mean monthly precipitation calculated from the CGD data set is considerable (see Figure 3), even though the model area is small in size and relatively flat. Especially in June and July there is a clear North-South gradient with 75-80 mm/month in the North of the area and 55-60 mm/month in the South.

### 3 Methodology

#### 3.1 Fitting of the weather generator

RainSim is fitted to daily and hourly statistics for each calendar month from the observed time series (SVK) to best reproduce features at both hourly and daily levels, as described by Burton et al. (2008; 2010<sup>a,b</sup>). A custom weighing scheme is used to support the features of rainfall that are important in the context of the present study. RainSim uses the Shuffled Complex Evolution fitting algorithm in combination with an objective function that normalises the fitting statistics (to avoid bias) for optimisation; furthermore, the algorithm is run thrice to avoid sub-optima (Burton et al., 2008). The statistics used for fitting the WG are:

- The mean daily precipitation intensity from the individual gauges (24 hour mean)

- 1 • The variance of the intensity of the daily and hourly observations from the  
2 individual gauges (1 hour and 24 hour variance)
- 3 • The skewness of the intensity of the daily and hourly observations from the  
4 individual gauges (1 hour and 24 hour skewness)
- 5 • The probability of dry days and of dry hours based on the observations from  
6 the individual gauges and with thresholds of 1.0 and 0.1 mm respectively as  
7 suggested by Burton et al. (2008).
- 8 • The lag-1 auto-correlation of the hourly precipitation intensity calculated  
9 from the observations at the individual gauges
- 10 • The cross-correlation between observations of hourly precipitation intensity  
11 at the individual gauges

12 A weighing scheme is created from general knowledge on rainfall and urban hydrology,  
13 which prioritizes rainfall features relevant for the present study. The chosen weighing scheme  
14 (see Table 3) favours the higher order moment statistics, variance and skewness, over the  
15 mean as the extreme characteristics of the simulated precipitation is prioritised. Furthermore,  
16 the cross-correlation and auto-correlation are given high weights to ensure a realistic  
17 representation of the spatio-temporal extent of the simulated precipitation. The different  
18 observation time series are furthermore weighted relative to each other according to the  
19 effective length of the time series to give more weight to longer time series. This is done to  
20 increase the data basis for cross-correlation analysis, utilising that a great deal of the short  
21 time series are from recent years and thus overlap in time, see Figure 2.

22 The standard fitting bounds suggested by Burton et al. (2008) are applied in the fitting  
23 procedure to ensure that the WG is fitted with values that are considered realistic by the  
24 model developers for a North European climate.

### 25 **3.2 Evaluation of simulated time series**

26 The evaluation of the simulated time series will be in line with previous studies such as  
27 Olsson and Burlando (2002), Cowpertwait (2006) and Molnar and Burlando (2008). This  
28 implies that simulated time series are not evaluated against the observations with the  
29 expectation of a perfect fit; the expectation is rather that the simulated series should resemble  
30 measured precipitation. In practise this is achieved by analysis of the statistics used in the  
31 fitting procedure and through analysis of statistics which are independent of the fitting  
32 statistics as will be outlined in Section 3.4.

1 For evaluation of all realisations of the WG the 60 grid cells closest to the observational  
2 gauges are extracted and evaluated point-wise with respect to all the fitting statistics as  
3 recommended by Burton et al. (2008). Furthermore, the WG is refitted to the simulated data  
4 sets to evaluate if the realisation is representative and results in model parameters that are  
5 comparable to the parameters estimated from the SVK observational data set.

6 Ten realisations of the WG, named WG1 to WG10, are used in this study. The actual  
7 simulation time is very short, but the process of writing data to text files for the complete grid  
8 takes long time. Also, the refitting of the WG data sets takes a long time to complete, making  
9 it a rather cumbersome approach, which limits the number of realisations evaluated in this  
10 study.

11 The refitted WG data is evaluated with respect to the fitting statistics,  $Y$ , through discussion of  
12 the density plots for the normalized error against the SVK data set:

$$13 \epsilon = \frac{Y_{WG} - Y_{SVK}}{Y_{SVK}} \quad (1)$$

Formatted: Font: Italic

Formatted: Font: Times New Roman,  
Not Italic

### 14 3.3 Perturbation of the weather generator with climate change signals

15 The fitted WG is perturbed with climate change signals by application of ~~climate~~-change  
16 factors,  $\alpha_{i,j,k}$ 's, to the ~~key~~-statistics,  $Y_{i,j,k}^{Present}$ 's, calculated from the SVK data set and used to  
17 fit the original WG for the present climate. In this manner new ~~key~~-statistics are produced for  
18 the future climate,  $Y_{i,j,k}^{Future}$ 's, as (Fowler et al., 2007, Burton et al., 2010b):

$$19 Y_{i,j,k}^{Future} = \alpha_{i,j,k} Y_{i,j,k}^{Present} \quad (+2)$$

20 where ~~One~~ climate change factor,  $\alpha$ , is calculated for each statistic,  $i$ , for each month,  $j$ , for  
21 each RCM,  $k$ . The change factors are calculated using the methodology introduced by Burton  
22 et al. (2010**b**) which includes transformations that ensure that the bounded statistics  
23 (probabilities of dry days and hours and auto-correlation) stays within their prescribed  
24 boundaries. No change factor is calculated for the cross-correlation as this statistic is  
25 described poorly by the RCMs (Gregersen et al., 2013).

### 26 3.4 Evaluation of extremes

27 Gregersen et al. (2013) compare extreme precipitation observations with RCM output. One  
28 issue is the difference in absolute magnitude of the extremes, which can partly be explained  
29 by the inherent difference between gridded data and point observations; another issue is the



1 spatial correlation structure of the extremes, where extremes calculated from RCM output  
2 have much too large spatial correlation distances at the sub-daily time scale. In this study, a  
3 simulated data set will be considered better than using RCM data directly for the specified  
4 purpose if it better resembles the observations with respect to both the absolute magnitude and  
5 the spatial correlation structure of the extremes.

6 The statistics used in this study to evaluate the WG's performance with respect to simulating  
7 extreme precipitation are based on the identification of independent rainfall events, as done  
8 when estimating intensity-frequency-duration relationships, see e.g. Madsen et al. (2002).  
9 Individual events are separated by dry periods equal to or longer than the chosen event  
10 duration (i.e. 1-hour events have at least 1 hour of dry weather between them and 24-hour  
11 events have at least 24 hours of dry weather between them) and the maximum averaged event  
12 intensities over the chosen durations are noted. Furthermore, the Peak over Threshold (POT)  
13 approach from Mikkelsen et al. (1996) and Madsen et al. (2002) is adopted with a global  
14 constant intensity threshold (i.e. Type I censoring) to derive the extreme event intensities for  
15 each gauge/grid point. In this study, extreme precipitation events are evaluated for 11 distinct  
16 durations of ~~between~~ 1, 2, 3, 4, 6, 8, 12, 24, 48, 72 and 120 hours with thresholds ranging  
17 (approximately log-linearly) from 7.6 to 0.34 mm/hour (the same as used by Gregersen et al.  
18 (2013) for the SVK data set). Three different event-based indices of extreme precipitation are  
19 evaluated as explained below.

### 20 3.4.1 Extreme event statistics

21 The return period of extreme events extracted from an observed or simulated rainfall time  
22 series is calculated using the California plotting position formula:

$$23 \quad T_m = \frac{T_{obs}}{m} \quad (23)$$

24 where  $T_m$  is the return period of the event (years) with rank  $m$  and  $T_{obs}$  is the observation  
25 period (years) of the time series.  $T_m$  is obviously affected by sampling variability and is  
26 biased, especially for large return periods. There are more elaborate methods to estimate  $T_m$   
27 than Eq (22), but we use Eq (22) here because it allows for comparing extreme value curves  
28 from multiple sites (including sampling variability and spatial variability) in a straightforward  
29 way.

30 A Generalised Pareto Distribution is fitted to extremes from every single time series:

$$z_T = z_0 + \mu \frac{1+\kappa}{\kappa} \left(1 - \left(\frac{1}{\lambda T}\right)^\kappa\right) \quad (34)$$

where:

- $z_T$  is the intensity for extreme event with return period  $T$
- $z_0$  is the threshold
- $\mu$  is the mean intensity of the extreme events
- $\lambda$  is the mean number of extremes per year
- $\kappa$  is the shape parameter
- $T$  is the return period

Based on  $z(T)$ 's intensity-duration-frequency curves are calculated for each data set.

For the climate change scenarios, change-climate factors for the intensity of the extreme events are calculated as a function of the return period for different  $T$ -year event durations. This is done as a simple ratio between the present and future levels for a given return period as

$$CF_T = \frac{z(T)^{future}}{z(T)^{present}} \quad (45)$$

### 3.4.2 Seasonality of extreme events

The seasonality of the extreme events is determined to further evaluate the realism of the behaviour of the WG. This is done to evaluate whether the WG data set constructed with individual monthly model parameters results in a realistic distribution of the extremes throughout the year. The determination is in practice performed by counting the number of extremes from the POT analysis that occur within each month for the SVK and WG data sets. These are then normalised and compared with a  $\chi^2$  test where the normalised counts  $C$  for the SVK data act as the expected values for the WG data set and where the summation is done over months giving a test statistic  $x$ :

$$x = \sum_{i=1}^{12} \frac{(C_i^{WG} - C_i^{SVK})^2}{C_i^{SVK}} \quad (56)$$

$x$  then follows a  $\chi^2$ -distribution with  $(12-1)(2-1) = 11$  degrees of freedom.

### 1 3.4.3 Unconditional spatial correlation of extremes

2 The unconditional spatial correlation,  $\rho$ , between the intensities of extreme events that are  
3 considered concurrent at different sites  $A$  and  $B$  is estimated. The methodology follows  
4 Mikkelsen et al. (1996) with the  $i$ 'th extreme intensity  $Z_{Ai}$  measured at site  $A$  being concurrent  
5 with the  $j$ 'th extreme event  $Z_{Bj}$  measured at site  $B$  if Eq. ~~6-7~~ is fulfilled. In this framework the  
6 precipitation process is considered to generate random occurrences of precipitation that are  
7 treated as correlated random variables,  $Z_A$  and  $Z_B$ , and two events are considered concurrent if  
8 they are overlapping in time or at most separated by a lag time  $\Delta t$ , which is introduced to  
9 account for the travel time of rain storms between sites.

$$10 \left\{ Z_{Ai}, Z_{Bj} \right\} : \left[ t_{si} - \frac{\Delta t}{2}, t_{ei} + \frac{\Delta t}{2} \right]_A \cap \left[ t_{sj} - \frac{\Delta t}{2}, t_{ej} + \frac{\Delta t}{2} \right]_B \neq \emptyset \quad (67)$$

11 Here  $t_s$  is the start times of the events and  $t_e$  is the end time of events. A lag time of  $\Delta t = 11$   
12 hours + the duration of the event is adopted in accordance with Gregersen et al. (2013). The  
13 introduction of this lag time, in combination with lack of knowledge of the movement  
14 direction of precipitation, implies that an individual event at one site can be correlated to more  
15 than one event at another site.

16 The unconditional covariance is then estimated by also accounting for non-concurrent  
17 extreme events at the two sites as:

$$18 \left\{ \text{cov}\{Z_A, Z_B\} = \text{cov}\{E\{Z_A|U\}, E\{Z_B|U\}\} + E\{\text{cov}\{Z_A, Z_B|U\}\} \right. \quad (78)$$

19 with  $U$  being a boolean operator taking the value of  $U = 1$  if events are concurrent and  $U = 0$   
20 otherwise. Finally, the unconditional correlation is obtained by division of Eq. (78) with the  
21 sample standard deviations of the two sites (Mikkelsen et al., 1996):

$$22 \left\{ \rho_{AB} = \frac{\text{cov}\{Z_A, Z_B\}}{\sqrt{\text{var}\{Z_A\} \text{var}\{Z_B\}}} \right. \quad (89)$$

23 The unconditional correlation values are grouped together in bins where the distance between  
24 the points considered are approximately the same, and an exponential model is fitted to  
25 describe the unconditional correlation's dependence on distance between sites using the e-  
26 folding distance measure as proposed by Gregersen et al. (2013).

## 4 Results and discussion

### 4.1 Fitting the weather generator

The WG converges to an optimum fit for the SVK and CGD data for all calendar months, resulting in a WG that is able to simulate realistic rainfall fields all year round. The parameter estimates (cf. Section 2.3) for the model fitted to SVK data, the parameter estimates for the model refitted to the 10 realisations of the WG (WG1 – WG10) and the used boundary values are given in Figure 4. All parameters vary over the course of the year, some more smoothly than others. Note that the  $\beta$  parameter (the parameter controlling the arrival time of cells after a storm origin) is constrained at its prescribed minimum value for four months (February, September, October and December). However, rain events can easily last for several days at these times of the year in Denmark, and this fitting artefact is therefore considered to have limited influence on those features of rainfall, which are of interest for this study. Figure 4 shows that all the refitted values are different and especially the  $\beta$  parameter does not always seem to follow the same structural pattern as for the SVK data set. As  $\beta^{-1}$  controls the arrival time of cells after storm origin it will be heavily dependent on the actual realisation of weather from the WG and this is not considered to be important for the realised extreme events. The  $\zeta$  parameter seems to be slightly biased in the same direction for all WGs.  $\zeta^{-1}$  controls the mean intensity of the rain cells and the difference in fit suggests that the rain in the WG data sets are slightly more intense during summer than what is seen in the SVK data set. Generally, the WG data sets however represent the SVK data set well.

The fitting statistics (cf. section 3.1) resulting from the direct analysis of the observations (SVK data set) and the simulations (WG data sets that are simulated based on fitting the WG to the SVK and CGD data) are compared in Figure 5 through the normalized error (Eq. 1) and directly in Table 4. Generally, the fit seems reasonable for all variables with distribution functions more or less centred on zero a mean of the normalized errors close to zero. For the moment statistics the WG data sets seem to be unable to reproduce the highest observed values to have a slight positive bias, and the variance and skewness distributions are also slightly positively skewed (Figure 5a-e). However the WG fit are still within the bounds reported for the SVK data set in Table 4, but for the bulk of observational points the fit is very good. The lag-1 auto-correlation and the probabilities of dry days and hours all seem to be fitted well even though the probability of dry days also seem to have some skewness in the error distribution. The probability of dry days is the only parameter that is significantly

1 ~~different~~ seems to differ between observations and WGs, ~~in the WGs compared to the SVK~~  
2 ~~indicate that the WG concentrates the precipitation on too few days.~~ Also, it seems that none  
3 of the WG realisations performs differently than the others with respect to reproduction of the  
4 fitting statistics. ~~and hence proving that the discrepancies observed in Figure 4 does not~~  
5 ~~seem to impede the use of the WGs as good proxies for observed precipitation.~~ ~~are of no~~  
6 ~~importance for the produced data product.~~

7 The cross correlation of the 1-hour intensities is shown ~~on~~ ~~in~~ Figure 6 for each month of the  
8 year. The 10 WG data sets seem to reflect the overall behaviour of the SVK data set very well  
9 and also capture most of the variability seen in the SVK data set. The very low correlations  
10 observed in the SVK data set for some “traces” of points, especially in March, October and  
11 November, are due to some time series only overlapping for very short time periods in recent  
12 years where the number of stations has increased dramatically (see Figure 2); hence the  
13 correlation is depending on only very few precipitation events. There is no evidence of a  
14 systematic pattern in these readings. Again, the difference between different WG realisations  
15 is very limited.

16 From Figures 5 and 6 the WG fit is considered satisfactory given the complex data set used  
17 and the purpose of this study. For analysis of extremes at event level this WG reproduces the  
18 features expected to have the highest influence on the produced extremes well.

#### 19 **4.2 Evaluation of extremes for present climate conditions**

20 For durations of 1 to 120 hours the extreme events are extracted from the SVK data set at  
21 each gauge and from the WG data sets in each grid cell closest to the SVK observation points  
22 and ranked according to return period (Eq. ~~23~~). Figure 7 shows intensity-duration-frequency  
23 curves estimated for WG realisation along with the SVK data set. For both ~~50-100~~ and 10-  
24 year events the WG data sets result in comparable extreme intensity values for all considered  
25 durations ~~well within the shown 68% confidence interval for the SVK IDF curve.~~

26 Figure 8 shows that the seasonal distribution of these extreme events is captured very well by  
27 the considered grids from the simulated WG data sets for all considered event durations. The  
28  $\chi^2$  tests furthermore confirm that there are no significant differences between distributions for  
29 the WG and the SVK data sets for all event durations.

30 Figure 9 shows the unconditional spatial correlation for the SVK and for the selected WG grid  
31 points calculated according to Eq. (~~89~~) and grouped in selected bins. Table ~~4-5~~ furthermore

1 compares the e-folding distances based on the fitted exponential models with a set of values  
2 calculated from RCM data representing a slightly larger area, taken from Gregersen et al.  
3 (2013).

4 Gregersen et al. (2013) show, using data from the whole of Denmark (range 0-350 km), that  
5 the spatial correlation pattern is not the same when considering output from climate models  
6 compared to SVK data as the climate model output maintains too long spatial correlation  
7 lengths at scales below approximately 150 km and 12 hours (see Table 45). Both [Figure](#)  
8 [9](#) and Table 4-5 indicate that the WG better reproduces the spatial correlation pattern  
9 of the SVK data within the spatial range (0-60 km) covered by the observations included in  
10 this study. The e-folding distances computed in this study for the SVK data set are somewhat  
11 lower than the ones calculated by Gregersen et al. (2013). This is a consequence of inclusion  
12 of fewer gauges and, most importantly, that the time series in the SVK data set for this study  
13 have been aggregated into hourly time series prior to the smoothing and POT analysis.  
14 Gregersen et al. (2013) conducted the smoothing and POT analysis directly on the original  
15 time series that have a one-minute resolution. The WG data sets represent the space-time  
16 features of precipitation of crucial importance for urban hydrology applications much better  
17 than the climate model output; the WG data set is considered realistic at this small-scale  
18 spatio-temporal resolution.

19 Overall, the results show that the WG is able to realistically simulate extreme precipitation  
20 statistics down to the hourly scale at a 2x2 km spatial resolution.

### 21 4.3 Perturbation of the weather generator with climate change signals from 22 RCMs

23 As the different realisations of the WG produce similar weather, only one 30-years realisation  
24 is used for perturbation with climate change signals from each of the RCMs. Furthermore, all  
25 grid cells are used for both present and future evaluations as no comparisons are made to the  
26 observational data.

27 For each RCM run and each statistic the ~~climate~~ change factors,  $\alpha_{i,j,k}$ 's, are calculated. They  
28 are primarily above 1 for the moment derived statistics ([Figure 10](#)~~Figure 10~~a-e) but the  
29 different RCM runs appear different. For the 24 hour mean ([Figure 10](#)~~Figure 10~~a) the  $\alpha_{i,j,k}$ 's  
30 are mostly above 1 with all RCM runs showing some months with values below 1 in an  
31 unsystematic pattern. For both the 24 and 1 hour variances ([Figure 10](#)~~Figure 10~~b and d) the

Formatted: English (U.K.)

Formatted: English (U.K.)

Formatted: English (U.K.)

Formatted: English (U.K.)

1 number of RCM runs and months that show a decrease is very limited and in general the  
2 variance will increase for all seasons. The HIRHAM RCP 8.5 simulation differs from the  
3 other RCM runs with very high  $\alpha_{i,j,k}$ 's for the summer months. The 24 and 1 hour skewness  
4 (Figure 10c and e) show more clear seasonality than the mean and variance with  
5 higher  $\alpha_{i,j,k}$ 's from May to September for all RCM runs clearly indicating a shift in the  
6 distribution of precipitation intensities towards more extremes. Again the HIRHAM RCP 8.5  
7 run stands out with very high  $\alpha_{i,j,k}$ 's for the 1 hour skewness for most of the year. This means  
8 that the extreme precipitation intensities are expected to be higher during summer and  
9 especially the sub-daily extremes for the HIRHAM RCP 8.5 perturbation could have very  
10 high intensities as a combination of a large increase in both variance and skewness will result  
11 in many severe precipitation events with a high mean intensity.

Formatted: English (U.K.)

12 For the lag-1 hour auto-correlation (Figure 10h) the  $\alpha_{i,j,k}$  are mostly below 1  
13 indicating more variations from one hour to the next and thus a possibility of more abrupt  
14 changes in the rainfall at the hourly level. For the probability of dry days and dry hours  
15 (Figure 10f and g) the pattern is less clear. The RCM simulations show some  
16 variation around 1 (approximately between 0.7 and 1.7) but do not agree with respect to  
17 season of these changes or their relative magnitude. This suggests that future rainfall will  
18 follow the same overall patterns as today but as all RCM runs have months with  $\alpha_{i,j,k}$  below 1  
19 there will also be more severe periods since the precipitation is concentrated on fewer days  
20 and hours. For instance, the peaks for the WRF RCP 8.5 perturbation in August for both  
21 probability of dry days and hours (Figure 10f and g) in combination with the  
22 increases in variance and skewness (Figure 10b to e) are expected to result in very  
23 severe extremes as the increased rainfall amount is expected to occur on fewer days. All in all,  
24 the  $\alpha_{i,j,k}$ 's indicate that for all RCM runs there will be more rainfall on average and it will be  
25 more variable resulting in more (and more severe) extremes events. This is in accordance with  
26 general findings from studies based on direct output from RCMs (Christensen and  
27 Christensen, 2007; Sunyer et al., 2014).

Formatted: English (U.K.)

Formatted: English (U.K.)

Formatted: English (U.K.)

#### 28 4.4 Changes in climate changed extremes from the weather generator

29 Calculating the climate change factors,  $CF^*$ s (Eq. 45), from the perturbed and original WG  
30 using the  $T$ -year event estimates calculated with Eq. 3-4 shows that despite the differences  
31 observed in the  $\alpha_{i,j,k}$  for the input statistics (Figure 10), the perturbation schemes  
32 based on RCM simulations modelling comparable climate change (HIRHAM SRES A1B,

Formatted: English (U.K.)

1 RACMO SRES A1B, HIRHAM RCP 4.5 and WRF RCP 4.5) result in similar changes to  
2 extremes after downscaling with the WG (Figure 11). Clearly, and as expected from  
3 the results in Figure 10, the HIRHAM RCP 8.5 perturbed WG results in a much  
4 more severe change in extreme precipitation than the other perturbation schemes for both 10  
5 and 100 year return periods. It is interesting that the WG perturbed with HIRHAM SRES  
6 A1B results in a rather stable  $CF$  in the range 1.35-1.55 with seemingly little dependence on  
7 return period and event duration, The WGs perturbed with RACMO SRES A1B, HIRHAM  
8 RCP 4.5 and WRF RCP 4.5 show similar  $CF$  values that are higher for 100-year extremes  
9 than for 10-year extremes but still not depend significantly on the event duration.

10 Both the HIRHAM RCP 8.5 and WRF RCP 8.5 perturbed WGs yield  $CF$  values that depend  
11 on the event duration with higher  $CF$  for short duration precipitation extremes. This indicates  
12 that this high-end scenario is changing the climate more drastically than the more moderate  
13 scenarios (SRES A1B and RCP 4.5) and that the observed extreme effects are not linearly  
14 scalable from moderate to high end scenarios. For event durations above 48 hours the  
15 different WGs yield similar  $CF$ 's, but surprisingly the high-end scenario WRF RCP 8.5  
16 perturbation scheme results in the smallest  $CF$  for the long duration events. This may indicate  
17 that the direct output from the RCMs underestimate the changes occurring at high spatio-  
18 temporal resolutions.

19 Despite the observed differences between WGs perturbed with different RCM runs and  
20 different forcing scenarios the results show an upwards change for all event durations (see  
21 Figure 11). The change seems to increase with the return period with a projected change  
22 factor in the order of 1.2-1.3 for  $T=10$  years and 1.4-1.5 for  $T=100$  years for the moderate  
23 scenarios (SRES A1B and RCP 4.5). Furthermore, the RCP 8.5 scenario perturbed WG runs  
24 suggest that short duration extreme events become relatively more severe compared to the  
25 WG runs perturbed with the other, moderate forcing scenarios.

#### 26 **4.5 Unconditional spatial correlation of climate changed $T$ -year events**

27 All the perturbed WG runs produce  $T$ -year precipitation events with reasonable spatial  
28 correlation structure (Figure 12, Table 56) includes calculated e-folding distances  
29 and it is noteworthy that the e-folding distance for present conditions is somewhat shorter for  
30 the full WG data set compared to the sub sets closest to the observations shown in Figure 9.  
31 The HIRHAM RCM and WRF RCM perturbed WG runs present similar results for all event

Formatted: English (U.K.)

Formatted: English (U.K.)



1 durations whereas the RACMO SRES A1B perturbed WG run yield slightly larger  
2 correlations lengths for the very short durations (~~Figure 12~~Figure 12a). Generally, all the  
3 perturbed WG runs have larger correlation lengths than for the present climate, suggesting  
4 that the WG implicitly expects that more severe events on average also results in events with  
5 a larger spatial extent. This behaviour has recently been observed by Kendon et al. (2014)  
6 using a high resolution regional climate model (1.5 km resolution). This difference, however,  
7 is limited, and in general the WG produces extremes with a spatial extent much closer to that  
8 of observations than RCMs. Online Resource 1 includes an animation of extreme  
9 precipitation events generated directly as output from the 25 km resolution RCM HIRHAM  
10 SRES A1B, the 8 km resolution RCM HIRHAM RCP 4.5 and the 2 km WG evaluated in this  
11 study. From these it is clear that the small-scale variability is much more pronounced for the  
12 WG output than for the output of the RCMs, but also that the WG output lacks rainfall  
13 movement. At the hourly scale this is not a problem for a catchment of the size presented in  
14 the Online Resource (same as shown in Figure 1).

15 Only few apparent effects are observed with respect to choice of RCM, GCM and RCM  
16 spatial resolution and it is not possible to detect any systematic patterns. The WG seems to  
17 produce robust results with respect to change in extreme precipitation due to climate change  
18 that are similar for similar climate forcing scenarios.

## 19 **5 Conclusions**

20 Precipitation time series based on high-resolution gauge measurements are presently used as  
21 input to design and analysis of urban water infrastructure, and time series representing future  
22 climates are needed in the future. Current RCMs operating at 25 and even 8 km spatial scales  
23 however yield too spatially correlated output that poorly represents the fine-scale precipitation  
24 features relevant for urban hydrology. The study indicate that statistical downscaling of  
25 precipitation output from RCMs using a stochastic weather generator (WG) is therefore a  
26 better solution.

27 This study demonstrates that the chosen Spatio-Temporal Neuman-Scott Rectangular Pulses  
28 weather generator (WG) fitted to a dense network of 60 rain gauges in a 40 by 60 km region  
29 simulates realistic extreme precipitation of relevance to urban hydrology. Output is generated  
30 at the 1 hour temporal scale at a 2 km spatial grid, which is finer than what previous studies  
31 using this WG have focused on. Even though urban hydrology literature claims that rain data  
32 are ideally needed at a time scale of minutes, the hourly scale chosen here can still be of much

1 use when assessing climate change impacts in urban hydrology as it is much finer than what  
2 regional climate models can currently provide.

3 The WG generally reproduces statistics of the observations such as mean, variance and  
4 skewness of the rainfall intensity distribution well at both the hourly and daily levels. It also  
5 produces realistic levels of lag-1 auto-correlation, cross-correlation between output at  
6 different grid points and probabilities of dry days and hours. Evaluating the WG from an  
7 urban hydrological engineering perspective yields the following conclusions:

- 8 • The extreme events of the simulated time series show realistic levels of  
9 intensity as well as a reasonable spatial variability for the full 60x40 km  
10 model area. Thus, the WG handles the large data set of spatially distributed  
11 observational input in a robust manner.
- 12 • The seasonal distribution of the extremes are not significantly different in  
13 the generated WG data sets compared to the observed SVK data set,  
14 implying that the applied procedure of individual monthly model fits results  
15 in a realistic seasonal behaviour of the WG.
- 16 • The spatial extent of the extreme events in the WG data set, as evidenced by  
17 the unconditional spatial correlation of extremes, is close to that of the  
18 observational SVK data set with e-folding distances in the same order of  
19 magnitude. This is much better than what is observed for Regional Climate  
20 Model (RCM) output at 25 and 8 km grid scale in previous studies.

21 This indicates that the WG is a good way to downscale spatio-temporal precipitation output  
22 from RCMs to relevant urban scales and that the simulated output can be used directly as  
23 input to urban hydrological models.

24 Output from six different RCM runs representing average to high emission scenarios are used  
25 to perturb the WG for different possible future climate scenarios. Two have a 25 by 25 km  
26 spatial resolution and four have a very high 8 by 8 km spatial resolution, and all RCM data  
27 sets are available at hourly temporal resolution. A clear increase in the magnitude of extreme  
28 precipitation is observed for all climate change perturbations of the WG.

29 This study highlights that different RCMs run with the same greenhouse gas emission  
30 scenario can result in different precipitation output and hence different CFs for perturbation of  
31 the WG. Despite these observed differences, downscaling with the WG results in similar  
32 extreme precipitation behaviour for similar emission scenarios.

1 Most perturbed WGs confirm that there is a more severe climate change signal for extreme  
2 events. The two WGs perturbed by the RCP 8.5 scenario show a more severe climate change  
3 signal for short-duration events. However, this finding is not shared by the other emission  
4 scenarios, suggesting that extreme precipitation at  $T$ -year event level is not scalable between  
5 emission scenarios. The spatial correlation structure of the WG output is slightly altered by  
6 the perturbation indicating a built-in correlation between intensity and spatial extent and  
7 suggesting that precipitation extremes in a future climate may have larger spatial extent than  
8 extremes in the present climate.

9

## 10 **Acknowledgements**

11 This work was carried out with the support of the Danish Council for Independent Research  
12 as part of the project “Reducing Uncertainty of Future Extreme Precipitation”, contract no.  
13 09-067455. The observational SVK data set was provided by the Water Pollution Committee  
14 of the Society of Danish Engineers. The Climate Grid Denmark (CGD) is a commercial  
15 product made freely available for research by the Danish Meteorological Institute. The  
16 authors also thank the Royal Netherlands Meteorological Institute, KNMI, and Erik van  
17 Meijgaard who kindly provided the RACMO data in a temporal resolution of 1 h, although  
18 this was outside the agreement of the ENSEMBLES project. The high temporal resolution  
19 HIRHAM/ECHAM data was provided by DMI. The high resolution regional climate model  
20 runs were carried out as part of the project RiskChange funded by the Danish Council for  
21 Strategic Research, contract no. 10-093894 (<http://riskchange.dhigroup.com>).

## 1 **References**

- 2 Arnbjerg-Nielsen, K. and Onof, C.: Quantification of anticipated future changes in high resolution  
3 design rainfall for urban areas. *Atmospheric Research*, 2(3) 350-363, doi:  
4 10.1016/j.atmosres.2009.01.014. 2009
- 5 Arnbjerg-Nielsen, K., Willems, P., Olsson, J., Beecham, S., Pathirana. A., Gregersen, I.B., Madsen,  
6 H., Nguyen, V-T-V.: Impacts of climate change on rainfall extremes and urban drainage systems: a  
7 review. *Water Science and Technology*, 68(1), 16-28. doi: 10.2166/wst.2013.251. 2013.
- 8 Bentsen, M., Bethke, I., Debernard, J. B., Iversen, T., Kirkevåg, A., Seland, Ø., Drange, H., Roelandt,  
9 C., Seierstad, I. A., Hoose, C., and Kristjánsson, J. E.: The Norwegian Earth System Model,  
10 NorESM1-M – Part 1: Description and basic evaluation of the physical climate. *Geoscientific Model  
11 Development*, 6, 687-720. doi: 10.5194/gmd-6-687-2013. 2013.
- 12 Berndtsson, R. and Niemczynowicz, J.: Spatial and temporal scales in rainfall analysis: Some aspects  
13 and future perspectives. *Journal of Hydrology*, 100: 293-313. doi: 10.1016/0022-1694(88)90189-8.  
14 1988
- 15 Burton, A., Kilsby, C. G., Fowler, H. J., Cowpertwait, P. S. P. and O'Connell, P. E.: RainSim: a spatial  
16 temporal stochastic rainfall modelling system. *Environmental Modelling and Software*, 23(12), 1356-  
17 1369. doi: 10.1016/j.envsoft.2008.04.003. 2008.
- 18 Burton, A., Fowler, H. J., Kilsby, C. G., and O'Connell, P. E.: A stochastic model for the spatial-  
19 temporal simulation of nonhomogeneous rainfall occurrence and amounts, *Water Resources Research*,  
20 46(11). doi:10.1029/2009WR008884. 2010a.
- 21 Burton, A., Fowler, H.J., Blenkinsop, S., and Kilsby, C.G.: Downscaling transient climate change  
22 using a Neyman-Scott Rectangular Pulses stochastic rainfall model, *Journal of Hydrology*, 381 (1-2)  
23 18-32, DOI: 10.1016/j.jhydrol.2009.10.031. 2010b.
- 24 Chen, J., Brissette, F. P., and Leconte, R.: A daily stochastic weather generator for preserving low-  
25 frequency of climate variability, *Journal of Hydrology*, 388, 480–490.  
26 doi:10.1016/j.jhydrol.2010.05.032. 2010.
- 27 Cowpertwait, P. S. P.: A Poisson-cluster model of rainfall: high-order moments and extreme values.  
28 *Proceedings of the Royal society A*, 454, 885-898. doi: 10.1098/rspa.1998.0191. 1998.
- 29 Cowpertwait, P. S. P.: A spatial-temporal point process model of rainfall for the Thames catchment,  
30 UK. *Journal of Hydrology*, 330(3-4), 586–595. doi:10.1016/j.jhydrol.2006.04.043. 2006.

Formatted: Font: Italic

Formatted: Font: Italic

1 Cowpertwait, P. S. P. and O'Connell, P. E.: A Regionalised Neyman-Scott Model of Rainfall with  
2 Convective and Stratiform Cells. *Hydrology and Earth System Sciences*, 1(1), 71-80. doi:  
3 10.5194/hess-1-71-1997. 1997.

4 Cowpertwait, P. S. P., Ocio, D., Collazos, G., de Cos, O. and Stocker, C.: Regionalised spatiotemporal  
5 rainfall and temperature models for flood studies in the Basque Country, Spain. *Hydrology and Earth  
6 System Sciences*, 17, 479–494. doi: 10.5194/hess-17-479-2013. 2013.

7 Christensen, O. B. and Christensen, J. H.: A summary of the PRUDENCE model projections of  
8 changes in European climate by the end of the century. *Climatic Change*, 81(1), 7-30. doi:  
9 10.1007/s10584-006-9210-7. 2007.

10 Christensen, O. B., Drews, M., Christensen, J. H., Dethloff, K., Ketelsen, K., Hebestadt, I., Rinke, A.:  
11 The HIRHAM Regional Climate Model, version 5( $\beta$ ). Danish Meteorological Institute Technical  
12 report 06–17. 2006.

13 Fowler, A. M. and Hennessy, K.J.: Potential impacts of global warming on the frequency and  
14 magnitude of heavy precipitation. *Natural Hazards* 11:283–303. doi:10.1007/BF00613411. 1995.

15 Fowler, H. J., Blenkinsop, S. and Tebaldi, C.: Review linking climate change modelling to impacts  
16 studies: recent advances in downscaling techniques for hydrological modelling. *International Journal  
17 of Climatology* 27, 1547–1578. doi: 10.1002/joc.1556. 2007.

18 Furrer, E. M. and Katz R. W.: Improving the simulation of extreme precipitation events by stochastic  
19 weather generators. *Water Resources Research*, 44(12). doi:10.1029/2008WR007316. 2008.

20 Gregersen I. B., Sørup H. J. D., Madsen H., Rosbjerg D., Mikkelsen P. S. and Arnbjerg-Nielsen K.:  
21 Assessing future climatic changes of rainfall extremes at small spatio-temporal scales. *Climatic  
22 Change*. 118(4), 783-797. doi: 10.1007/s10584-012-0669-0. 2013.

23 Hazeleger, W., Wang, X., Severijns, C., Ștefănescu, S., Bintanja, R., Sterl, A., Wyser, K., Semmler,  
24 T., Yang, S., van den Hurk, B., van Noije, T., van der Linden, E. and van der Wiel, K.: EC-Earth  
25 V2.2: description and validation of a new seamless earth system prediction model. *Climate Dynamics*  
26 39(11), 2611-2629. doi: 10.1007/s00382-011-1228-5. 2012.

27 Hundecha, Y., Pahlow, M. and Schumann, A.: Modeling of daily precipitation at multiple locations  
28 using a mixture of distributions to characterize the extremes. *Water Resources Research*, 45(12).  
29 doi:10.1029/2008WR007453. 2009.

30 Jørgensen, H. K., Rosenørn, S., Madsen, H. and Mikkelsen, P. S.: Quality control of rain data used for  
31 urban runoff systems. *Water Science and Technology*, 37(11), 113-120. doi: 10.1016/S0273-  
32 1223(98)00323-0. 1998.

- 1 Kendon, E. J., Roberts, N. M., Fowler, H. J., Roberts, M.J., Chan, S. C. and Senior, C.A. (2014)  
2 Heavier summer downpours with climate change revealed by weather forecast resolution model.  
3 *Nature Climate Change*, 4(7), 570-576.
- 4 Larsen, A. N., Gregersen, I. B., Christensen, O. B., Linde, J. J. and Mikkelsen, P. S.: Potential future  
5 increase in extreme precipitation events over Europe due to climate change. *Water Science and*  
6 *Technology*, 60(9), 2205-2216. doi: 10.2166/wst.2009.650. 2009.
- 7 Madsen, H., Mikkelsen, P. S., Rosbjerg, D. and Harremoes, P.: Regional estimation of rainfall  
8 intensity-duration-frequency curves using generalized least squares regression of partial duration  
9 series statistics. *Water Resources Research*, 38(11), 21-1-21-11. doi:10.1029/2001WR001125. 2002.
- 10 Madsen, H., Arnbjerg-Nielsen, K. and Mikkelsen, P. S.: Update of regional intensity-duration-  
11 frequency curves in Denmark: Tendency towards increased storm intensities. *Atmospheric Research*  
12 92(3), 343-349. doi: 10.1016/j.atmosres.2009.01.013. 2009.
- 13 Maraun, D., Wetterhall, F., Ireson, A. M., Chandler, R. E., Kendon, E. J., Widmann, M., Brienen, S.,  
14 Rust, H. W., Sauter, T., Themeßl, M., Venema, V. K. C., Chun, K. P., Goodess, C. M., Jones, R. G.,  
15 Onof, C., Vrac, M. and Thiele-Eich, I.: Precipitation downscaling under climate change: Recent  
16 developments to bridge the gap between dynamical models and the end user. *Reviews of Geophysics*  
17 48(3). doi: 10.1029/2009RG000314. 2010.
- 18 ~~Mayer, S., Maule, C., Sobolowski, S., Christensen, O., Sørup, H., Sunyer, M., Arnbjerg-Nielsen, K.,~~  
19 ~~and Barstad, I.: Identifying added value in high-resolution climate simulations over Scandinavia.~~  
20 ~~*Tellus A*, 67. doi:http://dx.doi.org/10.3402/tellusa.v67.24941. 2015.~~ Mayer, S., Maule, C. F.,  
21 ~~Sobolowski, S., Bossing, O. B., Sørup, H. J. D., Sunyer, M., Arnbjerg-Nielsen, K. and Barstad, I.:~~  
22 ~~Added value from high-resolution mini-ensemble climate simulations over Scandinavia? *Tellus A*.~~  
23 ~~accepted.~~
- 24 Meijgaard, E. v, Ulft, L. H. v, Berg, W. J. v d, Bosveld, F. C., Hurk, B. J. J. M. v d, Lenderink, G.,  
25 Siebesma, A. P.: The KNMI regional atmospheric climate model RACMO, version 2.1. Report no.  
26 302. KNMI Technical Report. 2008.
- 27 ~~1694(96)80009-6-1996.~~
- 28 Mikkelsen, P. S., Madsen, H., Rosbjerg, D. and Harremoes, P.: Properties of extreme point rainfall .3.  
29 Identification of spatial inter-site correlation structure. *Atmospheric Research*, 40(1), 77-98.  
30 doi:10.1016/0169-8095(95)00026-7. 1996.
- 31 Mikkelsen, P. S., Madsen, H., Arnbjerg-Nielsen, K., Jørgensen, H. K., Rosbjerg, D., and Harremoës,  
32 P.: A rationale for using local and regional point rainfall data for design and analysis of urban storm  
33 drainage systems. *Water Science and Technology*, 37(11), 7-14. 1998.

Formatted: Font: Italic

1 [Molnar, P., and Burlando, P.: Variability in the scale properties of high-resolution precipitation data in](#)  
2 [the Alpine climate of Switzerland. \*Water - Resources - Research\*, - 44\(10\), - W10404.](#)  
3 [doi:10.1029/2007wr006142. 2008.](#)

Formatted: Font: Italic

4 Nguyen, V.-T.-V., Nguyen, T-D. and Ashkar, F.: Regional frequency analysis of extreme rainfalls.  
5 *Water Science and Technology*, 45(2), 75-81. 2002.

6 [Olsson, J., and Burlando, P.: Reproduction of temporal scaling by a rectangular pulses rainfall model.](#)  
7 [\*Hydrological Processes\*, 16\(3\), 611–630. doi:10.1002/hyp.307. 2002.](#)

Formatted: Font: Italic

8 Olsson, J., Berggren, K., Olofsson, M., Viklander, M.: Applying climate model precipitation scenarios  
9 for urban hydrological assessment: a case study in Kalmar City, Sweden. *Atmospheric Research*,  
10 92:364–375. doi:10.1016/j.atmosres.2009.01.015. 2009.

11 Roeckner, E., Bäuml, G., Bonaventura, L., Brokopf, R., Esch, M., Giorgetta, M., Hagemann, S.,  
12 Kirchner, I., Kornblueh, L., Manzini, E., Rhodin, A., Schlese, U., Schulzweida, U. and Tompkins, A.:  
13 The atmospheric general circulation model ECHAM5: Model description. Max Planck Institute for  
14 Meteorology Rep. 349, 140 pp. 2003.

15 Rodriguez-Iturbe, I., Cox, D. R. and Isham, V.: Some models for rainfall based on stochastic point  
16 processes. *Proceedings of the Royal Society of London, Series A* 410, 269–288. doi:  
17 10.1098/rspa.1987.0039. 1987a.

18 Rodriguez-Iturbe, I., Febres de Power, B. and Valdes, J. B.: Rectangular pulses point process models  
19 for rainfall: analysis of empirical data. *Journal of Geophysical Research*, 92(8), 9645–9656. doi:  
20 10.1029/JD092iD08p09645. 1987b.

21 [Scharling, M.: \*klimagrid Danmark nedbør 10\\*10 km \(ver.2\) – metodebeskrivelse\*. Danish](#)  
22 [Meteorological Institute Technical report no 99-15. In Danish. 1999.](#)

Formatted: Danish

23 Scharling, M.: *Climate Grid Denmark*. Danish Meteorological Institute Technical report no 12-10.  
24 2012.

25 Schilling, W.: Rainfall data for urban hydrology: what do we need? *Atmospheric Research* 27, 5–22.  
26 doi: 10.1016/0169-8095(91)90003-F. 1991.

27 Skamarock, W., Klemp, J., Dudhia, J., Gill, D. and Barker, D.: A description of the Advanced  
28 Research WRF version 3. *NCAR Tech. Note NCAR/TN-475+ STR*, 113. 2005.

29 Sunyer, M. A., Gregersen, I. B., Rosbjerg, D., Madsen, H., Luchner, J., and Arbjerg-Nielsen, K.:  
30 Comparison of different statistical downscaling methods to estimate changes in hourly extreme  
31 precipitation using RCM projections from ENSEMBLES. *International Journal of Climatology*.  
32 doi:10.1002/joc.4138. 2014.

- 1 Sunyer, M. A., Madsen, H. and Ang, P. H.: A comparison of different regional climate models and  
2 statistical downscaling methods for extreme rainfall estimation under climate change. *Atmospheric*  
3 *Research*, 103. 129-128 doi:10.1016/j.atmosres.2011.06.011. 2012.
- 4 Sunyer, M. A., Madsen, H., Rosbjerg, D. and Arnbjerg-Nielsen, K.: A Bayesian Approach for  
5 Uncertainty Quantification of Extreme Precipitation Projections Including Climate Model  
6 Interdependency and Non-Stationary Bias. *Journal of Climate*, 27(18), 7113-7132 doi: 10.1175/JCLI-  
7 D-13-00589.1. 2014.
- 8 Sunyer, M. A., Sørup, H. J. D., Madsen, H., Rosbjerg, D., Christensen, O. B., Mikkelsen, P. S. and  
9 Arnbjerg-Nielsen K.: On the importance of observational data properties when assessing regional  
10 climate model performance of extreme precipitation. *Hydrological Earth System Science*. 17(11),  
11 4323-4337. doi: 10.5194/hess-17-4323-2013. 2013.
- 12 Tebaldi, C., and Knutti, R.: The use of the multi-model ensemble in probabilistic climate projections.  
13 *Philosophical Transactions Series A, Mathematical, Physical, and Engineering Sciences*, 365, 2053-  
14 2075. doi: 10.1098/rsta.2007.2076. 2007.
- 15 van der Linden, P., Mitchell, J. F. B. (eds): ENSEMBLES: Climate Change and its Impacts: Summary  
16 of research and results from the ENSEMBLES project. Met Office Hadley Center, Exeter. 2009.
- 17 van Vuuren, D. P., Edmonson, J., Kainuma, M., Riahi, K., Thomson, A., Hibbard, K., Hurtt, G. C.,  
18 Kram, T., Krey, V., Lamarque, J.-F., Masui, T., Meinshausen, M., Nakicenovic, N., Smith, S. J. and  
19 Rose, S. K.: The representative concentration pathways: an overview. *Climatic Change* 109(1-2), 5-  
20 31. doi: 10.1007/s10584-011-0148-z. 2011.
- 21 Verhoest, N. E. C., Vandenberghe, S., Cabus, P., Onof, C., Meca-Figuera, T. and Jameleddine, S.:  
22 Are Stochastic point rainfall models able to preserve extreme flood statistics? *Hydrological Processes*  
23 24, 3439-3445. doi: 10.1002/hyp.7867. 2010.
- 24 Vrac, M., Stein, M., and Hayhoe, K.: Statistical downscaling of precipitation through  
25 nonhomogeneous stochastic weather typing, *Climate Research*, 34, 169–184. doi:10.3354/cr00696.  
26 2007.
- 27 Waymire, E. and Gupta, V. K.: The mathematical structure of rainfall representations. I. A review of  
28 the stochastic rainfall models. *Water Resources Research*, 17(5), 1261-1272.  
29 doi:10.1029/WR017i005p01261. 1981.
- 30 Wilks, D. S. and Wilby, R. L.: The Weather generator game: a review of stochastic weather models.  
31 *Progress in Physical Geography*, 23(3), 329-357. doi:10.1177/030913339902300302. 1999.



- 1 Willems, P., Arnbjerg-Nielsen, K., Olsson, J. and Nguyen, V.-T.-V.: Climate change impact  
2 assessment on urban rainfall extremes and urban drainage: methods and shortcomings. *Atmospheric*  
3 *Research*, 103. 106-118. doi:10.1016/j.atmosres.2011.04.003. 2012.
- 4 Wood, A. W., Leung, L. R., Sridhar, V. and Lettenmaier, D. P.: Hydrologic Implications of Dynamical  
5 and Statistical Approaches to Downscaling Climate Model Outputs. *Climatic Change*, 62(1-3) 189-  
6 216. doi:10.1023/B:CLIM.0000013685.99609.9e. 2004.
- 7

1 Table 1 Main characteristics of the two observational data sets used in this study.

	<b>Type of data</b>	<b>Spatial data resolution</b>	<b>Temporal data resolution</b>	<b>Period</b>
<b>SVK</b>	Point observations	60 stations	Minute data	1979-2012
<b>CGD</b>	Gridded data	10 km grid	Daily data	1989-2010

2

1 Table 2 Regional Climate Model (RCM) runs from which precipitation output is used to  
 2 calculate perturbations schemes for the WG used in this study. All have a temporal resolution of  
 3 1 hour.

Name	RCM	GCM	Spatial resolution	Present period	Future period
<b>HIRHAM SRES A1B</b>	HIRHAM 5	ECHAM 5	25 km	1980-2009	2070-2099
<b>RACMO SRES A1B</b>	RACMO 2.1	ECHAM 5	25 km	1980-2009	2070-2099
<b>HIRHAM rcp 4.5</b>	HIRHAM 5	EC-EARTH	8 km	1981-2010	2071-2100
<b>HIRHAM rcp 8.5</b>	HIRHAM 5	EC-EARTH	8 km	1981-2010	2071-2100
<b>WRF rcp 4.5</b>	WRF 3	NorESM	8 km	1981-2010	2071-2100
<b>WRF rcp 8.5</b>	WRF 3	NorESM	8 km	1981-2010	2071-2100

4

1 Table 3 The relative weights used in the fitting procedure. \*All the cross-correlations of a gauge  
2 have equal weights that sum up to the value shown.

<b>Statistic</b>	<b>Relative weight</b>
<b>24 hour mean</b>	1
<b>24 hour variance</b>	3
<b>24 hour skewness</b>	6
<b>1 hour variance</b>	3
<b>1 hour skewness</b>	6
<b>1 hour auto-correlation</b>	6
<b>1 hour Cross-correlation</b>	6*
<b>Probability of dry day</b>	1
<b>Probability of dry hour</b>	1

3 |

1 Table 4 Comparison between observational (SVK) data and the simulated (WGs) statistics. Data  
 2 are averaged over the full course of the year and over the full model domain. For the SVK data  
 3 set the 50<sup>th</sup> percentile is reported as well as the 16<sup>th</sup> to 84<sup>th</sup> percentiles interval to emulate the  
 4 empirical standard deviation. For the WGs one central 50<sup>th</sup> percentile is reported across the ten  
 5 simulations.

	<u>24 hour mean</u> <u>(mm/day)</u>	<u>24 hour variance</u> <u>(mm<sup>2</sup>/day<sup>2</sup>)</u>	<u>24 hour skewness (-)</u>	<u>1 hour variance</u> <u>(mm<sup>2</sup>/hour<sup>2</sup>)</u>	<u>1 hour skewness (-)</u>	<u>Probability of dry</u> <u>days (-)</u>	<u>Probability of dry</u> <u>hours (-)</u>	<u>Lag-1 hour auto-</u> <u>correlation (-)</u>
<u>SVK</u> <u>(p50</u> <u>(p16-</u> <u>p84))</u>	<u>1.67</u> <u>(1.09-</u> <u>2.34)</u>	<u>12.6</u> <u>(6.05-</u> <u>32.9)</u>	<u>3.56</u> <u>(2.76-</u> <u>4.79)</u>	<u>0.117</u> <u>(0.0576-</u> <u>0.409)</u>	<u>8.93</u> <u>(6.73-</u> <u>15.1)</u>	<u>0.718</u> <u>(0.667-</u> <u>0.770)</u>	<u>0.934</u> <u>(0.914-</u> <u>0.947)</u>	<u>0.572</u> <u>(0.422</u> <u>-</u> <u>0.654)</u>
<u>WGs</u> <u>(p50)</u>	<u>1.60</u>	<u>14.9</u>	<u>4.04</u>	<u>0.151</u>	<u>10.4</u>	<u>0.812</u>	<u>0.945</u>	<u>0.578</u>

6  
7

- Formatted: Caption
- Formatted: English (U.S.)
- Formatted Table
- Formatted: Subtitle;Table 1, Indent: Left: 0 cm, Right: 0 cm
- Formatted: Font: (Default) Arial, Not Bold
- Formatted: Subtitle;Table 1
- Formatted: Font: (Default) Arial, Not Bold
- Formatted: Font: (Default) Arial, Not Bold
- Formatted: Font: (Default) Arial, Not Bold
- Formatted: Subtitle;Table 1, Left
- Formatted: Font: (Default) Arial, Not Bold
- Formatted: Font: (Default) Arial, Not Bold
- Formatted: Font: (Default) Arial, Not Bold
- Formatted: Font: (Default) Arial, Not Bold
- Formatted: Font: (Default) Arial, Not Bold
- Formatted: Font: (Default) Arial, Not Bold
- Formatted: Subtitle;Table 1
- Formatted: Font: Not Bold
- Formatted: Subtitle;Table 1, Left
- Formatted: Font: Not Bold
- Formatted: Font: Not Bold
- Formatted: Font: Not Bold
- Formatted: Font: Not Bold
- Formatted: Font: Not Bold
- Formatted: Font: Not Bold
- Formatted: Font: Not Bold
- Formatted: Font: Not Bold
- Formatted: Font: Not Bold
- Formatted: Font: Not Bold

1 | Table 54 e-folding distances for the SVK and WG maximum averaged intensities of extremes for  
 2 | 1, 6, 12 and 24 hours duration, based on the fitted exponential models (cf. Figure 8) as well as  
 3 | for a regional climate model (HIRHAM/ECHAM) from the study by Gregersen et al. (2013) for  
 4 | comparison. \*Values from Gregersen et al. (2013).

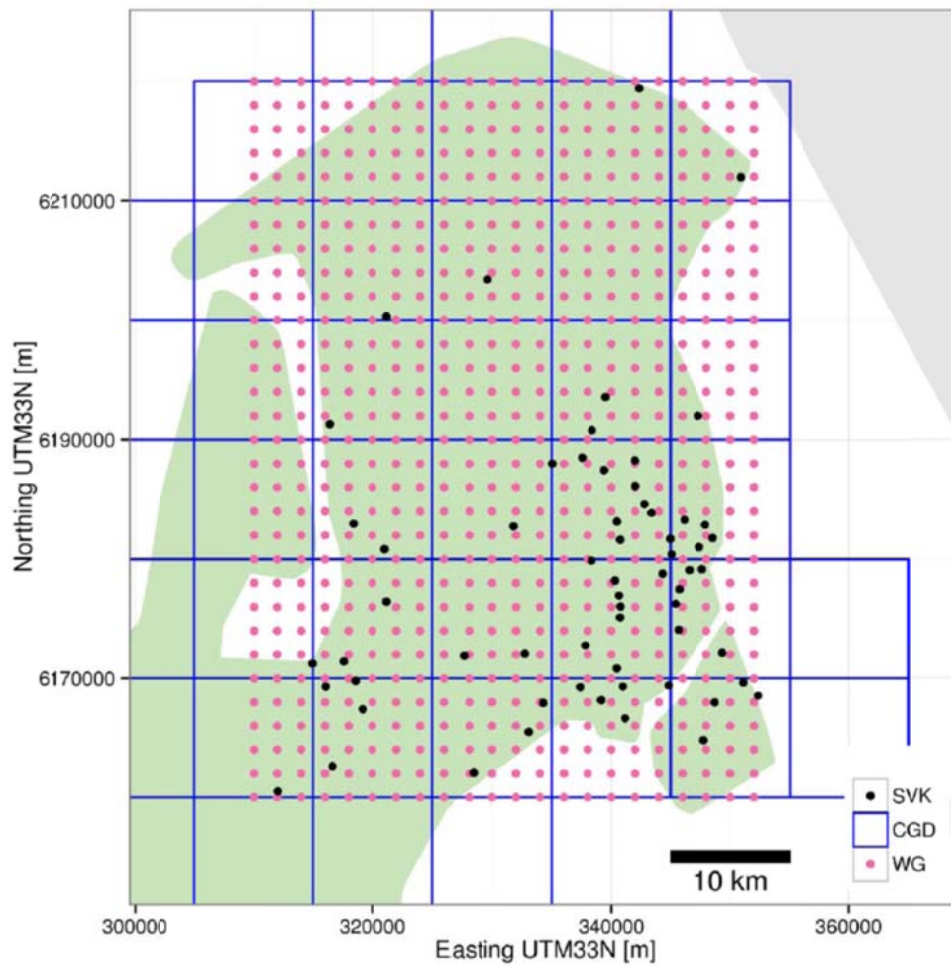
<b>e-folding distance [km]</b>	<b>1 hour</b>	<b>6 hour</b>	<b>12 hour</b>	<b>24 hour</b>
<b>SVK</b>	3.5	5.5	7.3	8.0
<b>WGs</b>	7.1 – 9.9	9.1 – 14	9.5 – 16	10 – 28
<b>HIRHAM/ECHAM*</b>	56	48	48	54

5  
6

1 | Table 6.5 e-folding distances for all aggregation periods for all WG output.

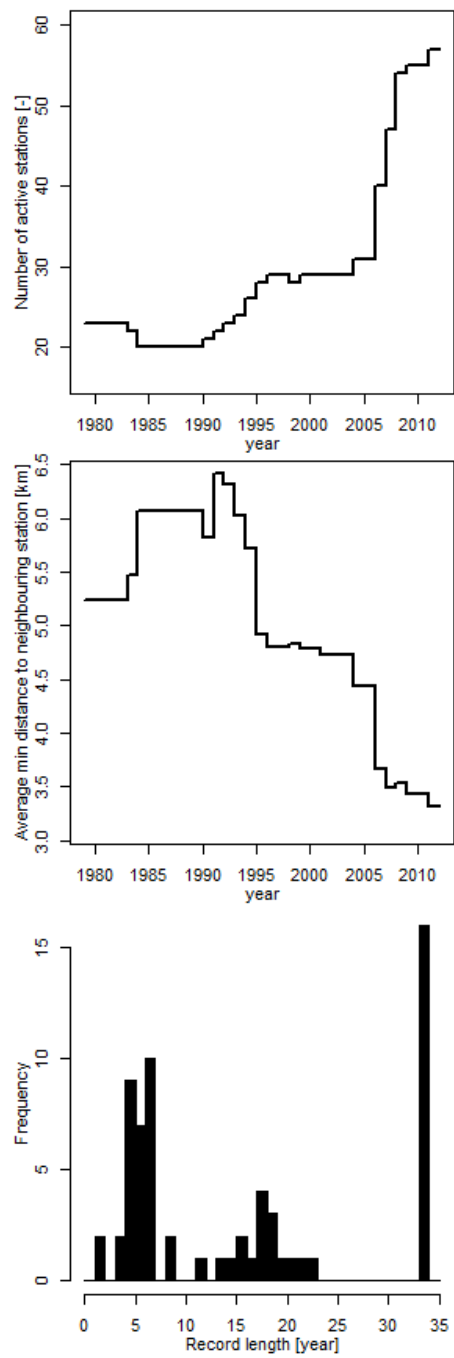
e-folding distance [km ]	Aggregation period			
	1 hour	6 hour	12 hour	24 hour
<b>WG – Present Climate</b>	3.9	5.0	4.9	5.0
<b>WG – HIRHAM SRES A1B</b>	5.2	7.4	7.7	8.1
<b>WG – RACMO SRES A1B</b>	7.3	9.7	9.1	8.4
<b>WG – HIRHAM rcp 4.5</b>	5.2	8.4	8.7	8.8
<b>WG – HIRHAM rcp 8.5</b>	4.6	7.7	9.3	9.0
<b>WG – WRF rcp 4.5</b>	5.1	9.1	9.3	11.5
<b>WG – WRF rcp 8.5</b>	4.9	9.4	9.9	10.2

2

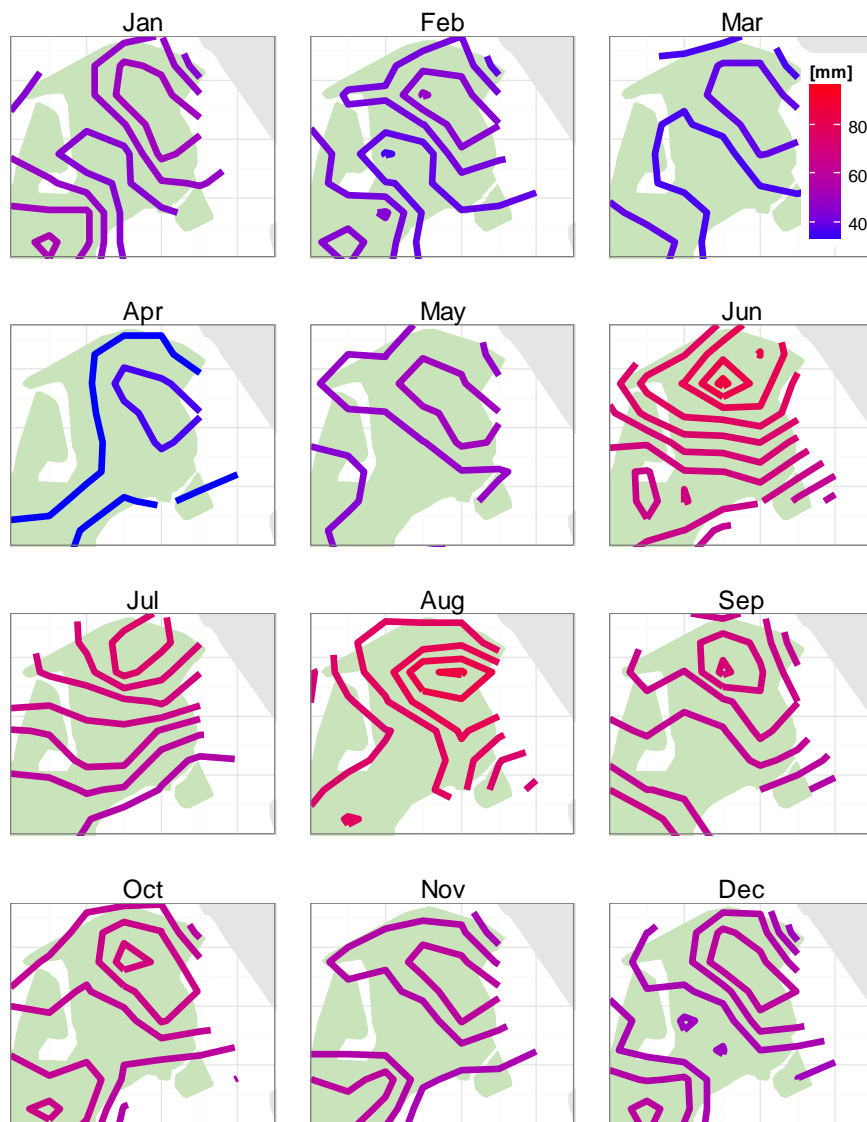


2  
 5 Figure 1 Locations of the rain gauges (SVK), the gridded data set (CGD) and extent of the  
 5 modelled grid (WG) in the North-Eastern part of Zealand (Denmark) including Copenhagen in  
 7 the South-Eastern part of the map where the concentration of SVK gauges is highest.

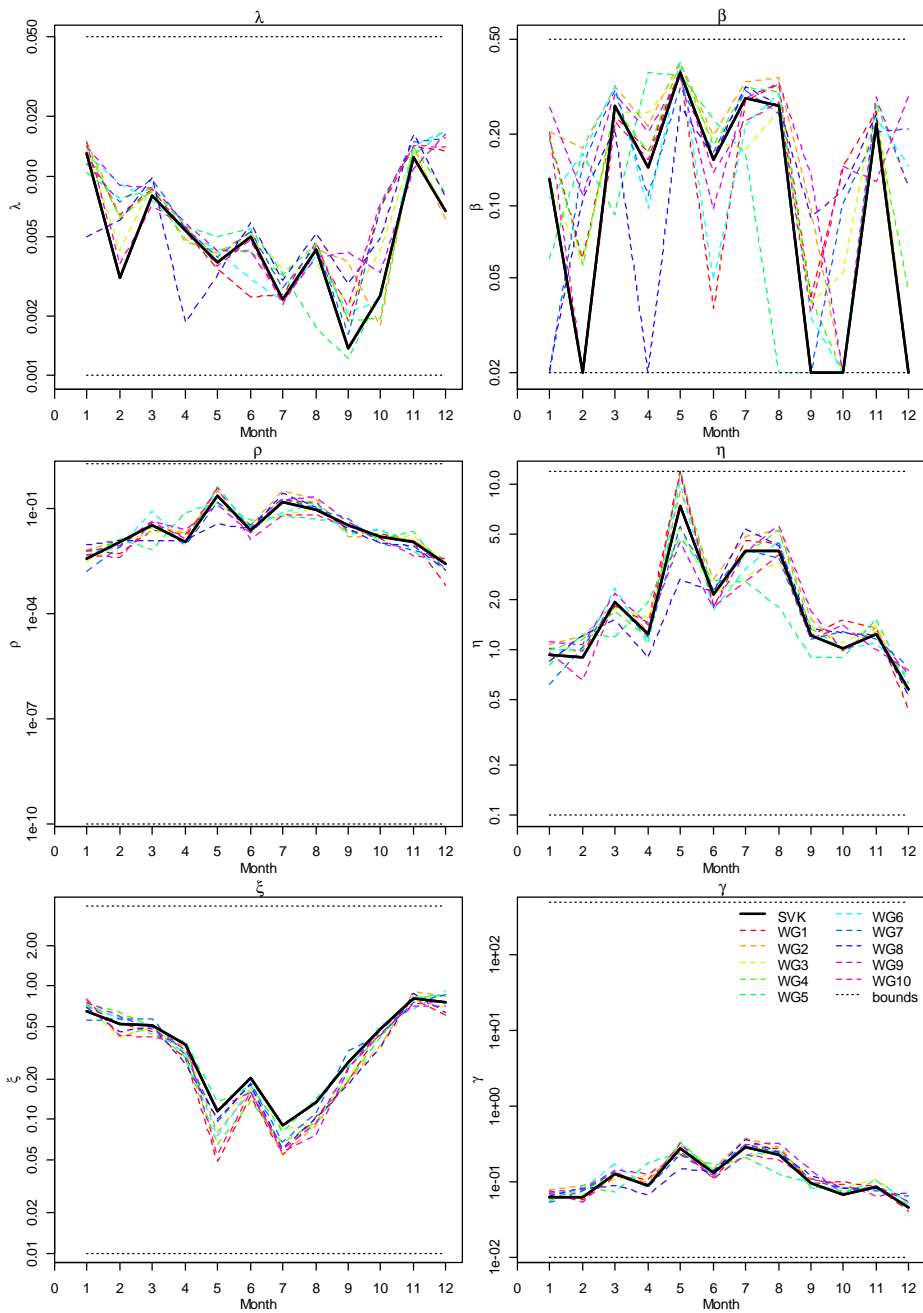




1  
 2 Figure 2 Temporal development in (top) the number of stations in the SVK data set and (middle)  
 3 the average distance between closest neighbouring stations, and (bottom) the distribution of  
 4 record lengths.

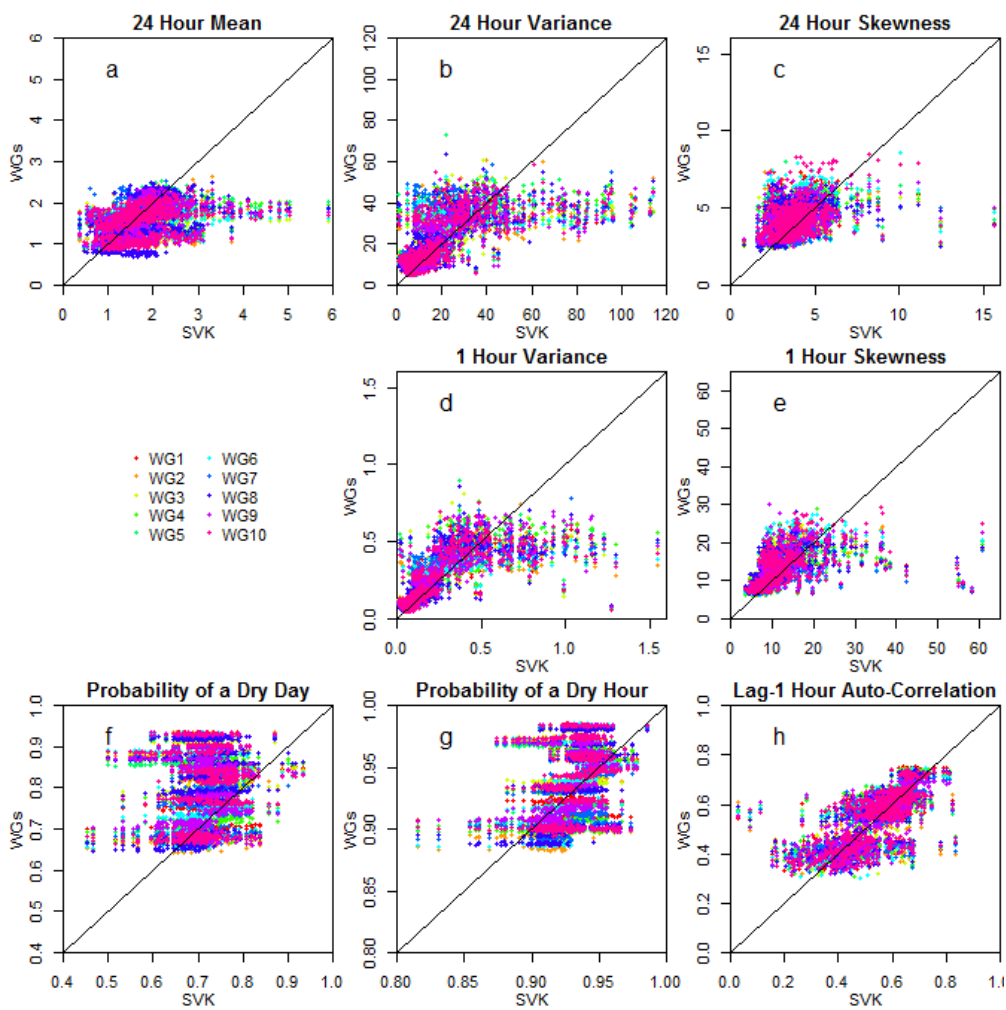


1  
 2 | Figure 3 Spatial variation of the mean monthly precipitation calculated from the CGD data set  
 3 | for the model area. Isohyets are 3 mm between.

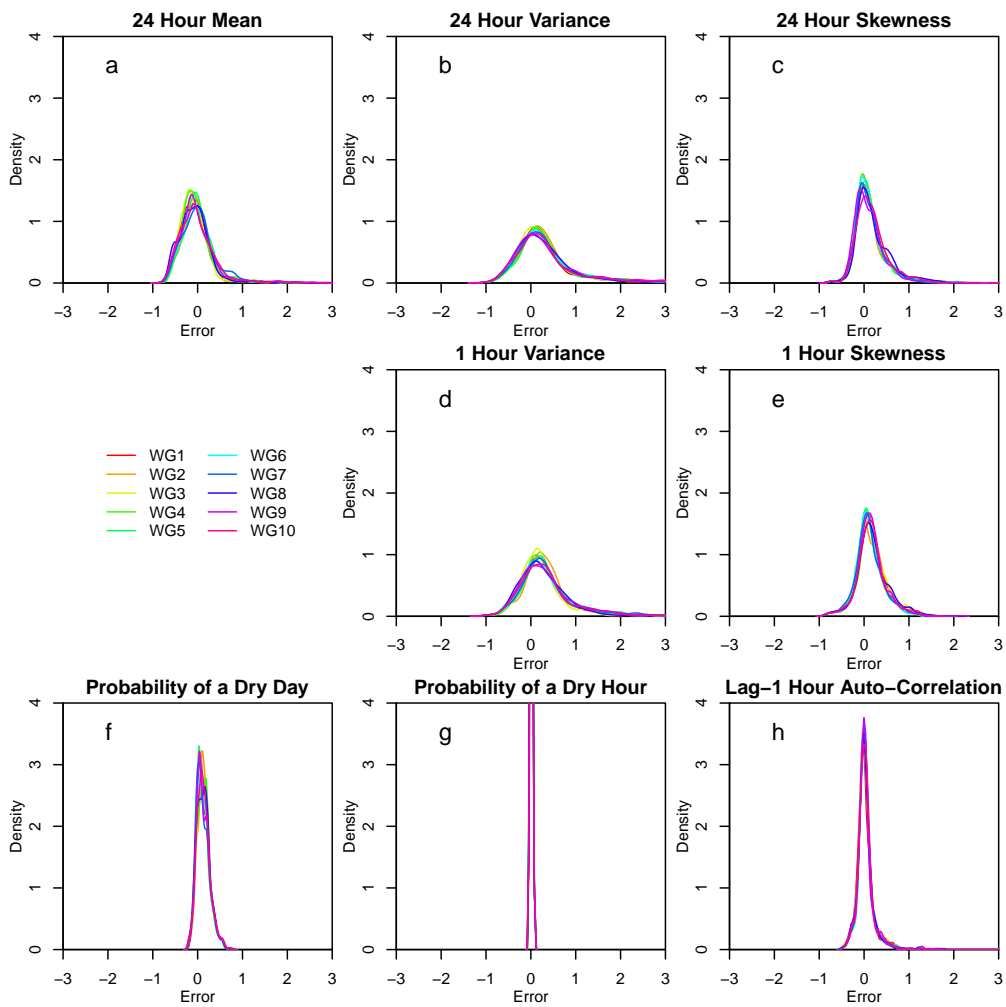


1  
 2 Figure 4 Monthly variation of the model parameters estimated from the SVK data set and from  
 3 the simulated 10 WG data sets. Upper and lower fitting bounds are shown in light grey.

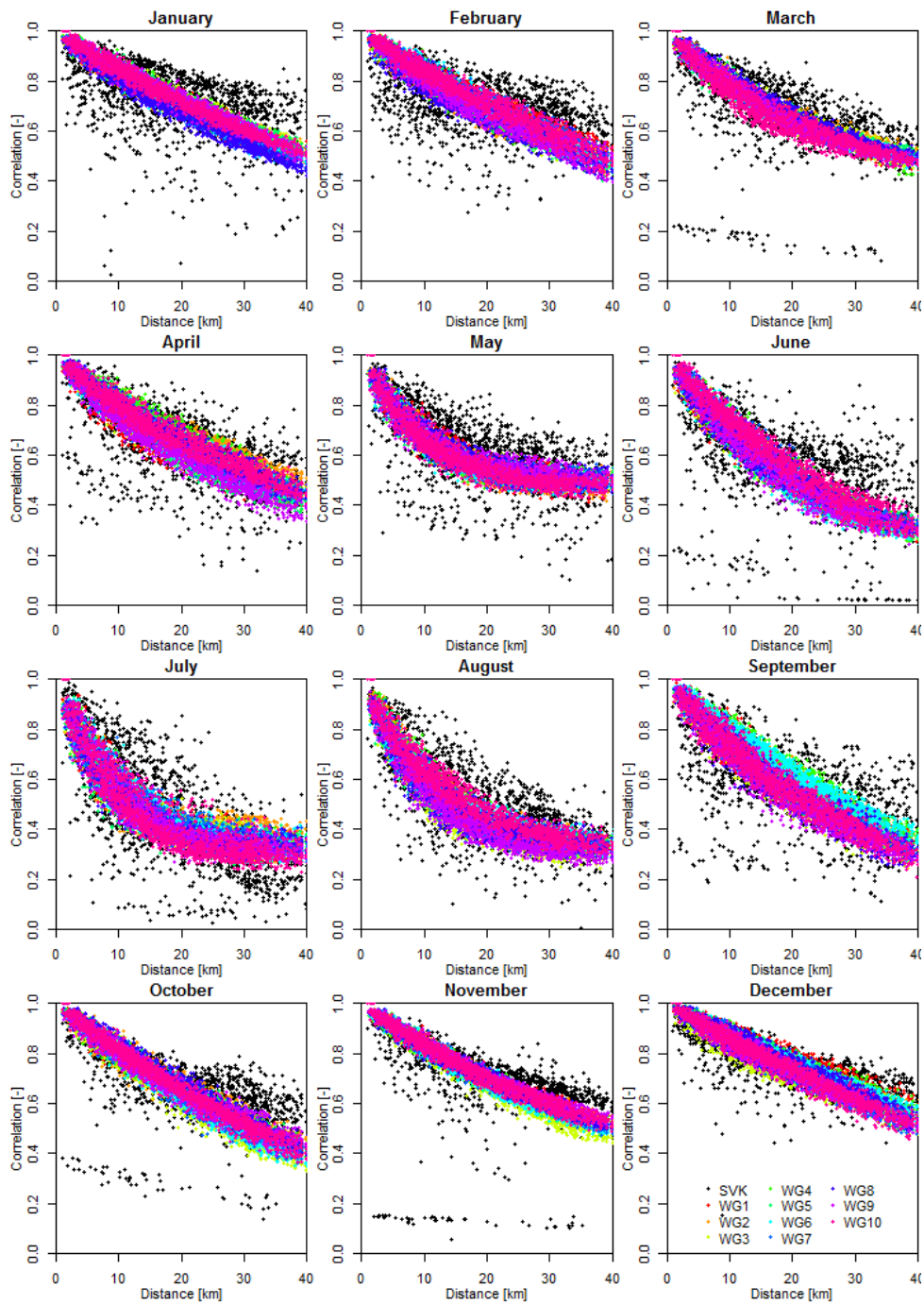
1



2

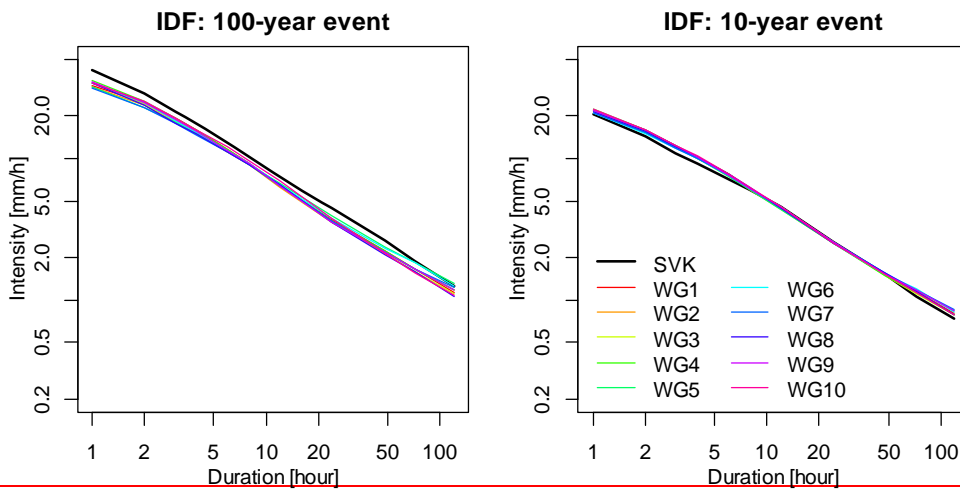


1  
 2 **Figure 5** ~~Fitting statistics~~ Density plots for the normalized error between the WG and the SVK  
 3 data sets, calculated from the SVK data set (observations) and WG (simulated) data set.

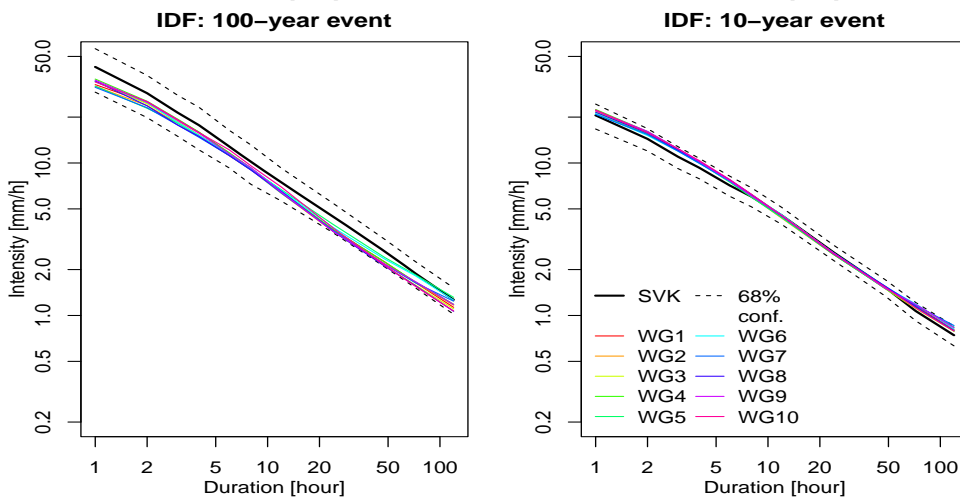


1  
 2 Figure 6 Variation of cross-correlation of the 1 hour intensity with distance between pairs of  
 3 gauges in the SVK data set (black dots) and grid points in the WG data set (coloured dots).

1

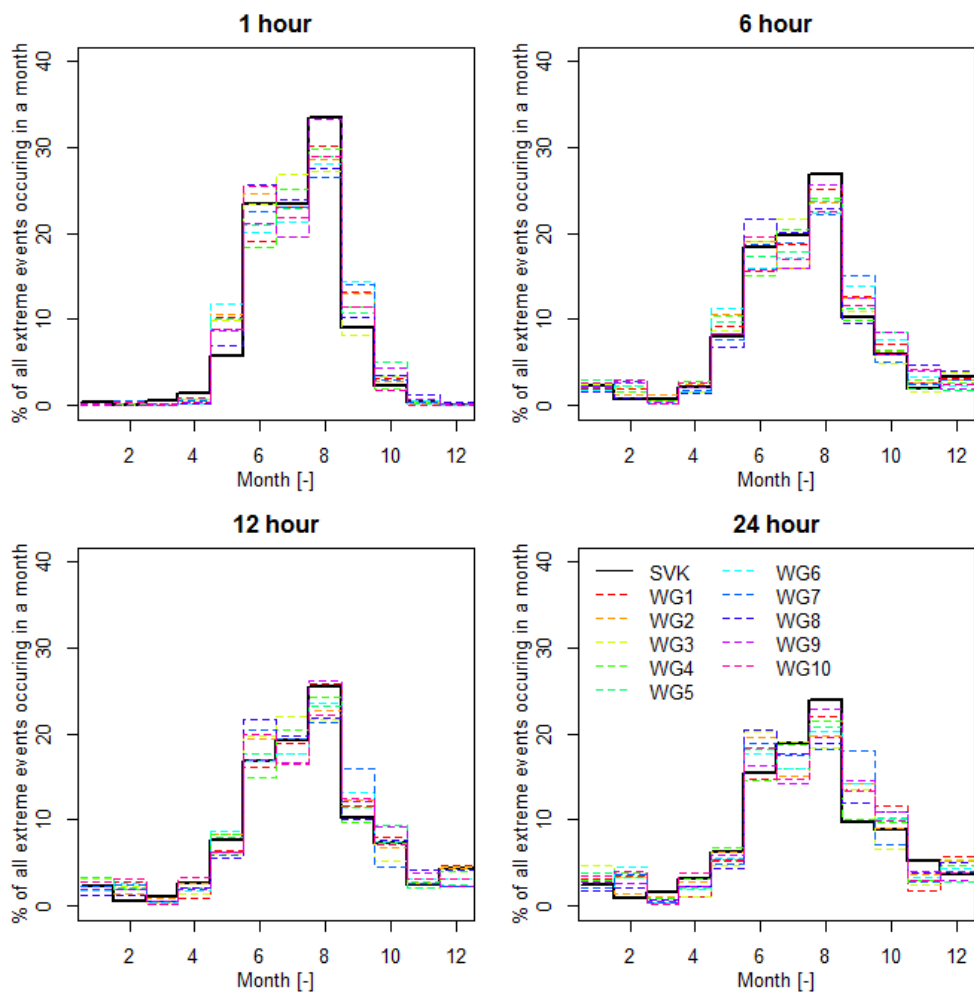


2



3 Figure 7 Mean intensity-duration-frequency curves for 100 and 10 year return periods calculated  
4 from the SVK data set and for all 10 WG realisations. [68% confidence interval for the SVK data](#)  
5 [set.](#)

1

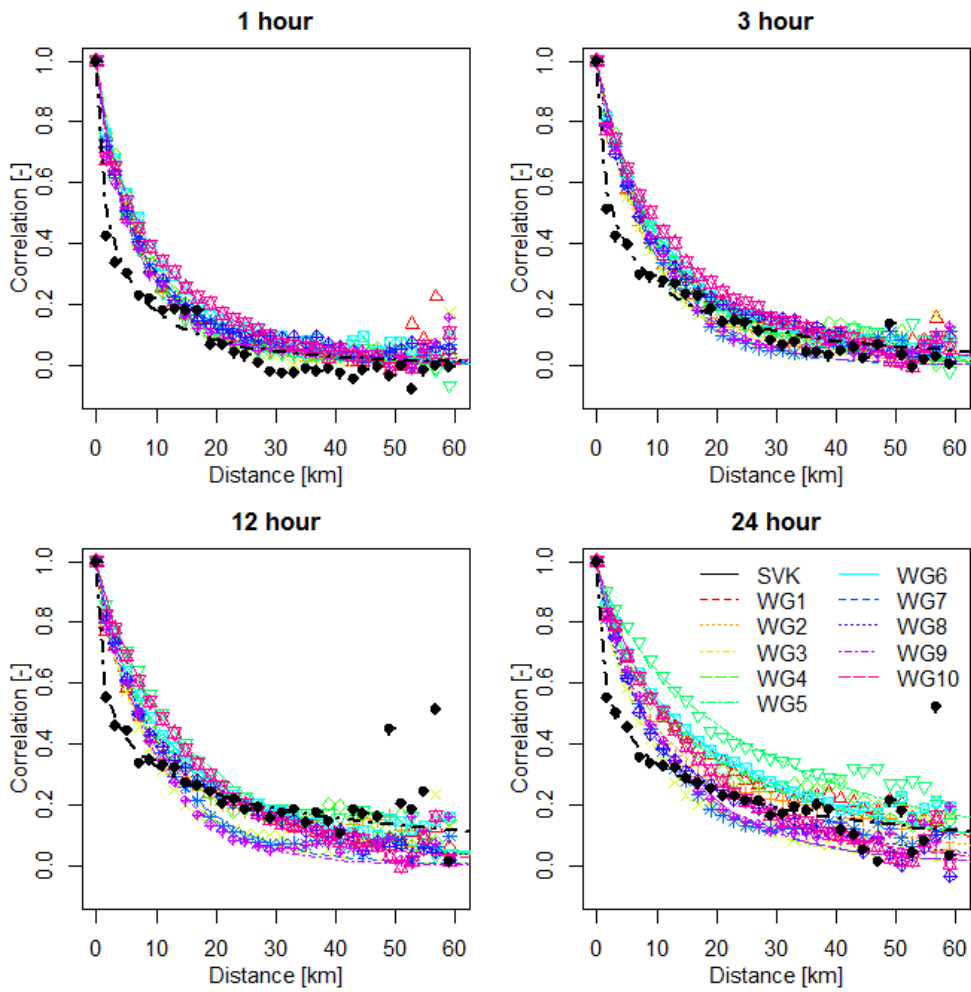


2

3 Figure 8 Monthly variation for 1, 6, 12 and 24-hour durations of the frequency of extreme events  
4 in the SVK and WG data sets.

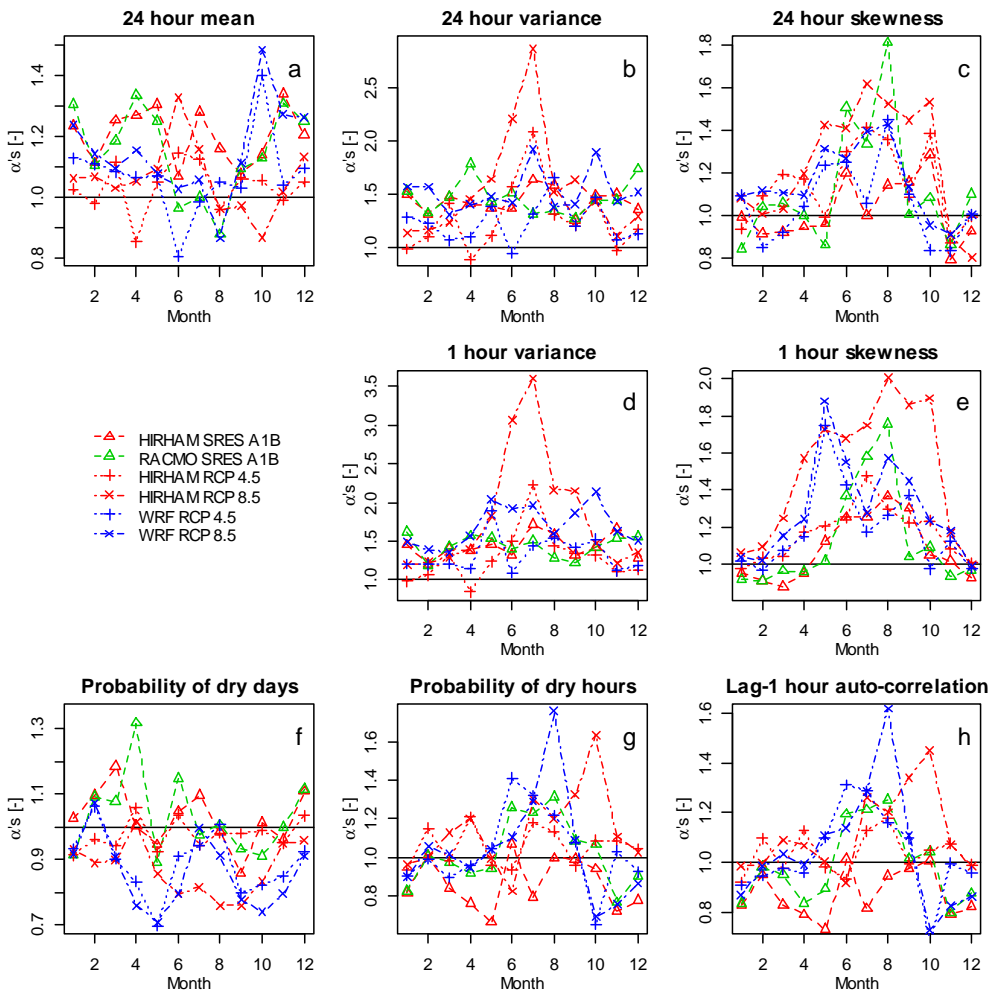


1

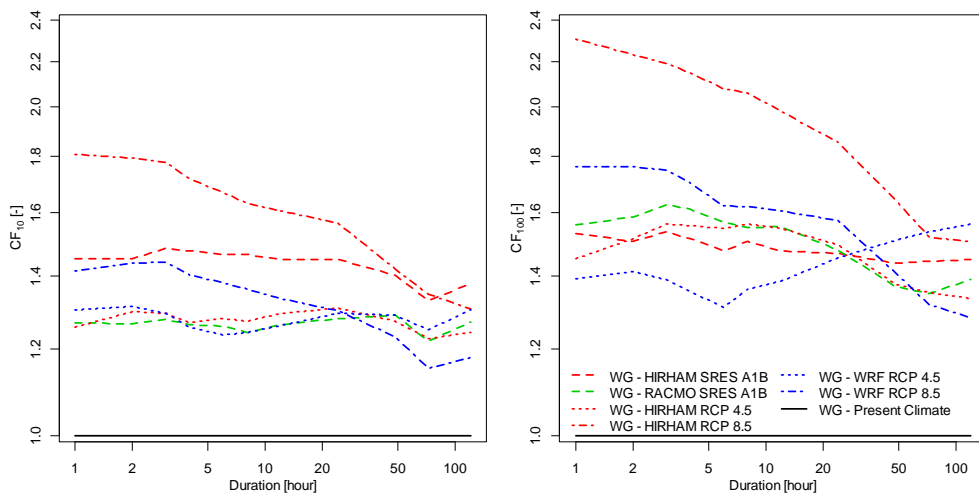


2

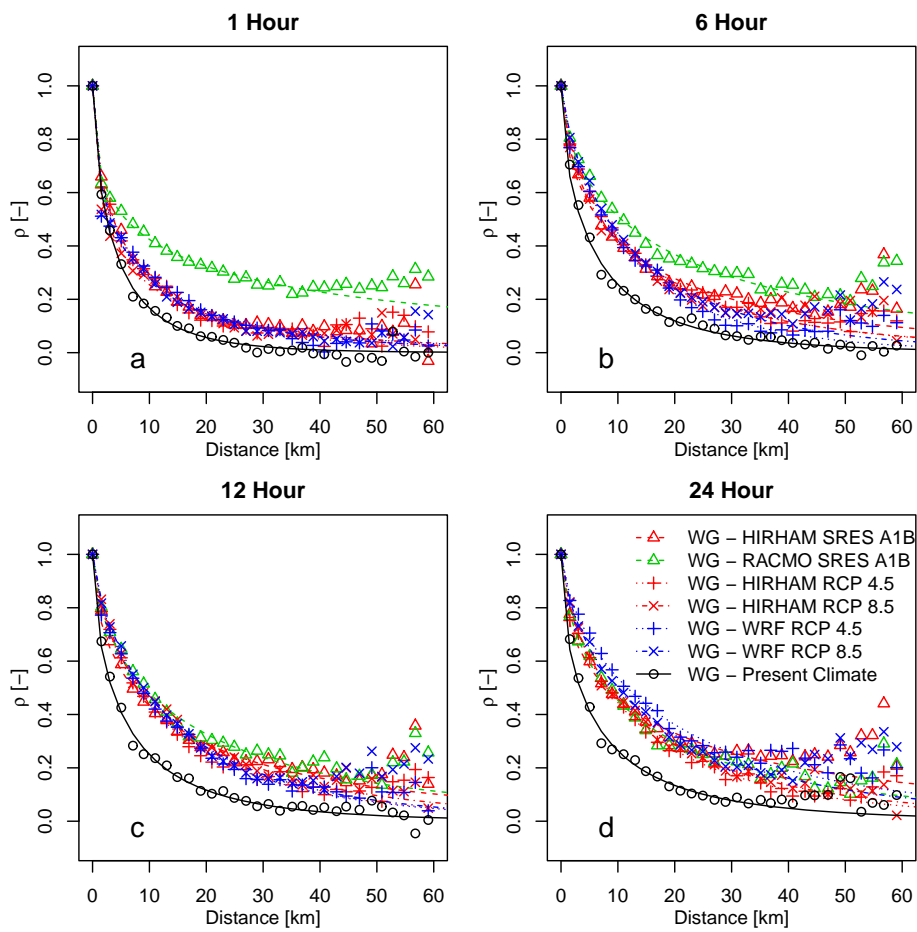
3 Figure 9 Unconditional spatial correlation for the SVK and WG data sets, calculated from  
4 maximum averaged intensities of extreme events for 1, 6, 12 and 24 hours duration. Fitted  
5 exponential models that highlight overall tendencies are shown.



1  
 2 | Figure 10 Climate-Change factors,  $\alpha's$ , calculated on a monthly basis for each statistic and each  
 3 RCM. Each set of  $\alpha's$  from an RCM act as a perturbation scheme for the WG.



1  
 2 | Figure 11 Climate ~~change~~ factors for different return periods for the different perturbed WG  
 3 runs.  $T=10$  years (left) and  $T=100$  years (right).



1  
 2 Figure 12 The unconditional spatial correlation of all  $T$ -year events for perturbed WG output for  
 3 event durations of 1, 6, 12 and 24 hours.